Silent Synapses Dictate Cocaine Memory Destabilization and Reconsolidation

William J. Wright[1,*], **Nicholas M. Graziane**[1,3,*], **Peter A. Neumann**[1], **Peter J. Hamilton**[4], **Hannah M. Cates**[4], **Lauren Fuerst**[1], **Alexander Spenceley**[1], **Natalie MacKinnon-Booth**[1], **Kartik Iyer**[1], **Yanhua H. Huang**[2], **Yavin Shaham**[5], **Oliver M. Schlüter**[1], **Eric J. Nestler**[4], **Yan Dong**[1,2]

[1]Departments of Neuroscience, University of Pittsburgh, Pittsburgh, PA 15260

[2]Department of Psychiatry, University of Pittsburgh, Pittsburgh, PA 15260

[3]Departments of Anesthesiology and Perioperative Medicine and Pharmacology, Penn State College of Medicine, Hershey, PA, 17033

[4]Nash Family Department of Neuroscience and Friedman Brain Institute, Icahn School of Medicine at Mount Sinai, New York, NY 10029

[5]Behavioral Neuroscience Branch, Intramural Research Program, National Institute on Drug Abuse, National Institutes of Health, Bethesda, Maryland 20892

Abstract

Cocaine-associated memories are persistent, but, upon retrieval, become temporarily destabilized and vulnerable to disruptions, followed by reconsolidation. To explore the synaptic underpinnings for these memory dynamics, we studied AMPA receptor (AMPAR)-silent excitatory synapses, which are generated in the nucleus accumbens by cocaine self-administration, and subsequently mature after prolonged withdrawal by recruiting AMPARs, echoing acquisition and consolidation of cocaine memories. We show that, upon memory retrieval after prolonged withdrawal, the matured silent synapses become AMPAR-silent again, followed by re-maturation ~6 hr later, defining the onset and termination of a destabilization window of cocaine memories. These synaptic dynamics are controlled by Rac1, with decreased and increased Rac1 activities opening and closing, respectively, the silent synapse-mediated destabilization window. Preventing silent synapse re-maturation within the destabilization window decreases cue-induced cocaine seeking. Thus, cocaine-generated silent synapses constitute a discrete synaptic ensemble dictating the dynamics of cocaine-associated memories and can be targeted for memory disruption.

Corresponding Address: Dr. Yan Dong, Dept. Neuroscience, Univ. of Pittsburgh, A210 Langley Hall / 5th & Ruskin Ave, Pittsburgh, PA 15260, yandong@pitt.edu, Phone: 412-624-3140.
*These authors contributed equally to the work

Keywords

silent synapse; cocaine; memory; reconsolidation; nucleus accumbens

Introduction

Consuming drugs of abuse produces drug-associated memories, which promote subsequent drug seeking and relapse[1,2]. Similar to other forms of memories[3], previously formed and consolidated drug memories can be retrieved upon re-exposure to cues associated with prior drug experience[4]. Upon retrieval, drug-related memories are transiently destabilized and become susceptible to disruption; the memories are then reconsolidated and become stable again[5,6]. Without knowing precise neuronal substrates underlying drug memories and their dynamics, aggressive but nonspecific amnestic manipulations, such as protein synthesis inhibition or beta-adrenergic receptor inhibition, within, but not outside of, the destabilization window effectively compromise drug memories and reduce subsequent drug seeking in rodent models[5–7]. However, nonspecific manipulations with more tolerable regimens fail to demonstrate consistent anti-relapse efficacy in human drug users[8–10]. These findings highlight the therapeutic potential of utilizing the memory destabilization window for anti-relapse treatments, but also call for the need to identify precise neuronal and molecular substrates encoding the dynamics of drug memories.

Synapses are likely the basic cellular units encoding memory traces. In search of a specific set of synapses encoding cocaine memories, we focused on nucleus accumbens (NAc) medium spiny neurons (MSNs), which are essential in acquiring and maintaining many forms of addiction-related memories, including cue-induced cocaine seeking, a behavioral readout driven by cue-associated cocaine memories[2]. The function of NAc MSNs is driven by excitatory synapses arising from several cortical and subcortical projections, with each input thought to mediate specific responses. Amongst such heterogeneous synapses emerge a unique population, which is generated *de novo* by cocaine experience, and is thus cocaine-specific. These synapses are formed within several NAc projections at low levels, but have common cellular features that distinguish them from other synapses. Namely, they are nascent, immature excitatory synapses that contain NMDA receptors (NMDARs) without stable AMPA receptors (AMPARs), and are thus AMPAR-silent[11–15]. After generation by cocaine self-administration, these silent synapses mature over time by recruiting calcium-permeable AMPARs (CP-AMPARs), and this maturing and strengthening process results in further enhancement, or incubation, of cue-induced cocaine seeking[16–18]. These results led to our hypothesis that the functional states of cocaine-generated silent synapses dictate the dynamics of cocaine-associative memories.

To test this hypothesis, we examined the role of NAc silent synapses in retrieval-induced destabilization and subsequent reconsolidation of cocaine memories. We trained rats in the cocaine self-administration procedure to establish cue-associative cocaine memories. Cue re-exposure, after prolonged drug withdrawal, induces retrieval and destabilization of cocaine memories. Coincidently, the matured cocaine-generated synapses become AMPAR-silent and weakened again for ~6 hr, and then re-matured and re-strengthened thereafter. These

synaptic dynamics, which define the onset and termination of retrieval-induced destabilization of cocaine memories, respectively, were controlled by the small GTPase Rac1 and involved bidirectional synaptic trafficking of CP-AMPARs. Rac1- and CP-AMPAR-based manipulations of silent synapse dynamics during, but not outside of, the 6-hr destabilization window decreased subsequent cue-induced cocaine seeking. These findings indicate that the functional states of cocaine-generated silent synapses dictate key aspects of cocaine memories, and can be targeted to manipulate cocaine memories and reduce cocaine relapse.

Results

Memory retrieval re-silences cocaine-generated synapses

We trained rats to self-administer cocaine, during which each intravenous infusion was paired with a light cue to form cocaine-cue associations. Consistent with our previous studies[16–18], rats acquired cue-associated cocaine memories after 5 days of self-administration, manifested by cue-induced cocaine seeking on withdrawal day 1. This cue-induced cocaine seeking "incubated" during drug abstinence[19] and became significantly greater after 45 days of withdrawal (Fig.1a–c). Thus, cue-associated cocaine memories are formed during drug self-administration training and strengthened/consolidated during prolonged drug withdrawal.

To assess silent synapses after cocaine memory formation and consolidation, we performed the minimal stimulation assay to estimate the percentage (%) of silent synapses among all sampled synapses in NAc shell (NAcSh) MSNs (Fig.1d,e). As demonstrated previously[12,15], if silent synapses are present in the set of recorded synapses, the failure rate in response to minimal stimulation at +50 mV is lower than that at −70 mV, and based on the differential failure rates, the % silent synapses can be estimated (Fig.1e) (see Methods). After 1 day of withdrawal from cocaine self-administration, the % silent synapses in NAcSh MSNs was significantly increased (Figs.1f–h,S1a–c). After prolonged (45 days) withdrawal, the % silent synapses decreased to control levels (Figs.1h,S1d–g). Our previous studies demonstrate that this decrease is partially due to the maturation and synaptic strengthening process, during which cocaine-generated synapses recruit CP-AMPARs and become unsilenced, contributing to the enhancement of cue-induced cocaine seeking after withdrawal[16,18]. This maturation is confirmed in our randomly sampled synapses; application of naspm (200 μM), a selective CP-AMPAR antagonist, restored the % silent synapses to the high levels observed after 1 day of withdrawal from cocaine self-administration (Figs.1h,S1h). Thus, cocaine self-administration generates new silent synapses, which subsequently mature after withdrawal via incorporation of CP-AMPARs, potentially contributing to the formation and consolidation of cocaine memories.

We next examined cue-induced retrieval and destabilization of cocaine memories. After 45 days of withdrawal from cocaine self-administration, we briefly (10 min) re-exposed the rats to cocaine-associated cues through an extinction session in the same operant chambers to reactivate and destabilize cocaine memories[5]. Immediately after cue re-exposure, the rats were analyzed for silent synapses in the NAcSh (Fig.1i). Cue re-exposure had no effect on the % silent synapses in rats previously trained with saline self-administration, indicating

that, without the cocaine-cue pairing, re-exposure to the light cue does not generate new synapses in the NAcSh (Figs.1j,m,S1i,j). However, the % silent synapses was increased in cocaine-trained rats with cue re-exposure compared to cocaine-trained rats without cue re-exposure (Figs.1k,m,S1i–q). The magnitude of this cue re-exposure-induced increase in % silent synapses was comparable to the increase induced by CP-AMPAR inhibition in cocaine-trained rats without cue re-exposure (Figs.1k,m,S1r). Since the cocaine-generated silent synapses mature by recruiting CP-AMPARs, we speculated that cue re-exposure-induced silent synapses are the mature cocaine-generated synapses after losing CP-AMPARs. Consistent with this speculation, inhibiting CP-AMPARs did not further increase the % silent synapses in cocaine-trained rats after cue re-exposure (Fig.1k–m).

While cue re-exposure did not generate new silent synapses in saline-trained rats (Figs. 1j,m,S1i,j), it may do so in cocaine-trained rats, similar to what occurs 1 day after cocaine self-administration. Generation of new silent synapses after cocaine experience involves synaptic insertion of GluN2B-containing NMDARs[12,20]. This was confirmed in our current experiments, in which NMDAR-mediated EPSCs in NAcSh MSNs exhibited increased sensitivity to the GluN2B-selective antagonist Ro256981 (200 nM) after 1 day withdrawal from cocaine self-administration (Fig.1n,S2a,b). On withdrawal day 45, the sensitivity of NMDAR EPSCs to Ro256981 declined to low levels (Fig.1o,S2c,d), suggesting that GluN2B NMDARs had been replaced with other NMDAR subtypes, which is consistent with the maturation of nascent synapses[21]. Importantly, cue re-exposure did not alter the low sensitivity of NMDARs to Ro256981 in cocaine-trained rats (Fig.1o), indicating that cue re-exposure did not trigger GluN2B-mediated *de novo* generation of silent synapses.

While GluN2B NMDARs were not changed by cue re-exposure in cocaine-trained rats, we detected internalization of CP-AMPARs. CP-AMPARs conduct minimal current at depolarized potentials[22], and can thus be detected by an increased inward rectification. In saline-trained rats, very low levels of CP-AMPARs are expressed at excitatory synapses on NAcSh MSNs, reflected as a linear I-V relationship of AMPAR EPSCs (Fig.1p,q). After 45 days of withdrawal from cocaine, AMPAR EPSCs become inwardly rectifying (Fig. 1p,q,S2e,f), indicative of CP-AMPAR incorporation to cocaine-generated synapses, as observed previously[16,18,23]. Cue re-exposure, however, normalized this rectification (Fig. 1p,q), suggesting removal of CP-AMPARs. Taken together, these results support a scenario of CP-AMPAR internalization-mediated re-silencing of matured silent synapses.

Retrieval-induced memory destabilization lasts ~6 hr before reconsolidation[4,24]. The dynamics of NAcSh silent synapses exhibited similar time course after cue re-exposure (Fig. 1r). Specifically, the % silent synapses remained high 2 or 4 hr after cue re-exposure, but returned to low levels after 6 hr (Figs.1s–v,S1m–s). At the 6-hr time point, inhibition of CP-AMPARs by naspm restored the high % silent synapses (Figs.1q,v), suggesting that the cue-re-silenced synapses re-mature by re-insertion of CP-AMPARs. Thus, the already matured silent synapses are re-silenced and weakened via internalization of CP-AMPARs upon cue re-exposure, and then re-matured 6 hr later. Thus, re-silencing and subsequent re-maturation of silent synapses follow the general time course of retrieval-induced destabilization and reconsolidation of cocaine memories.

The morphology of dendritic spines is correlated with the maturational state of glutamatergic synapses[25]. In NAcSh slices, we filled MSNs with Alexa 594 dye and imaged their secondary dendrites, which receive dense glutamatergic inputs (Fig.2a). NAcSh dendritic spines can be categorized into at least four subtypes: i) mushroom-like spines; ii) long-thin spines; iii) filopodia-like spines; and iv) stubby spines (Fig.2b) (see Methods)[20]. It is thought that mushroom-like spines represent mature synapses enriched in AMPARs, while long-thin and filopodia-like spines are relatively immature synapses with few or no AMPARs[25]. This relationship is supported by our previous studies examining cocaine-induced silent synapses in the NAcSh[20]. Due to their morphological and functional similarity, we combined long-thin and filopodia-like spines for data interpretation.

Similar to previous studies[20], on withdrawal day 1 after cocaine self-administration, the density of total spines was increased compared to saline-trained rats (Fig.S3a,b). This increase was primarily attributable to an increase in thin spines (Fig.S3c–g) that likely correspond to newly generated silent synapses. We also observed a small increase in the density of stubby spines (Fig.S3e), but given their low basal density and small contribution (~4%) to the total spine density change, their role in generation of silent synapses was considered to be minimal. On withdrawal day 45, the total spine density remained higher in cocaine-trained rats compared to saline-trained rats (Fig.2c,d,S3i–l). However, the density of thin spines in cocaine-trained rats returned to levels comparable to saline-trained rats (Fig. 2f). In contrast, the density of mushroom-like spines was increased in cocaine-trained rats (Fig.2e). The density of stubby spines was also slightly higher in cocaine-trained rats compared to saline-trained rats (Fig.2g). These spine patterns are consistent with the notion that cocaine-generated silent synapses mature and stabilize by recruiting AMPARs after 45 days of withdrawal.

After 45 days of withdrawal from cocaine self-administration, cue re-exposure did not alter the density of total spines, such that they remained high, comparable to cocaine-trained rats without cue re-exposure (Fig.2c,d). However, under these conditions, the density of mushroom-like spines decreased to lower levels, similar to saline-trained rats (Fig.2c,e). This decrease coincided with an increase in the density of thin spines (Fig.2c,f). Stubby spines were unaffected by cue re-exposure (Fig.2c,g). The simultaneous downshift of mushroom-like spines and upshift of thin spines suggest that some mature synapses return to a weakened, immature state, consistent with the notion that matured silent synapses are re-silenced after cue re-exposure. Furthermore, 6 hr after cue re-exposure, the densities of mushroom-like and thin spines returned to levels similar to the cocaine-trained rats without cue re-exposure, with no change in the density of total spines (Fig.2d–g). Thus, the weakened spines re-mature by the end of the destabilization window, corresponding to re-maturation of silent synapses and memory reconsolidation.

The diameter of spine heads can be used as an additional measure of synaptic strength complementary to the above morphological classification[26]. After 45 days of withdrawal from cocaine self-administration, the mean diameter of spine heads was increased compared to saline-trained rats (Fig.2h). Following cue re-exposure, the mean diameter of spine heads decreased to saline control levels (Fig.2h), suggesting synaptic weakening or re-silencing. However, 6 hr after cue re-exposure, the mean diameter of spine heads returned to the level

of cocaine-trained rats without cue re-exposure (Fig.2h), suggesting re-strengthening or re-maturation of synapses.

Based on the above results, we hypothesized that the states of NAc silent synapses, including their generation, maturation, re-silencing, and re-maturation, contribute to the formation, consolidation, retrieval-induced destabilization, and reconsolidation of cocaine memories, respectively (Fig.2i). We tested this hypothesis in the experiments described below.

Synapse re-silencing destabilizes cocaine memories

To determine the role of silent synapse dynamics in destabilization and subsequent reconsolidation of cocaine memories, we adopted a manipulation to prevent re-maturation of silent synapses after cue re-exposure by preventing re-insertion of CP-AMPARs (Fig.3a). Specifically, the small peptide TGL can bind to the C-terminus of GluA1 subunits to disrupt synaptic insertion of GluA1-containing AMPARs, which are the predominant population of cocaine-induced CP-AMPARs[2,27]. We conjugated TGL and its mutant control peptide AGL with a TAT sequence to allow intracellular delivery *in vivo*. To verify the efficacy of this peptide, we induced a subtype of long-term potentiation (LTP) in the hippocampal CA1 (Fig.S4a), whose expression primarily relies on synaptic insertion of GluA1 AMPARs[28,29]. Pre-incubation of hippocampal slices with TGL, but not AGL, prevented this GluA1 AMPAR-dependent LTP (Fig.S4a), validating this peptide-based approach.

We infused TGL or AGL (30 μM/side) into the NAcSh of rats ~2 hr after cue re-exposure on withdrawal day 45 (Fig.3b), conditions under which silent synapses re-emerged in cocaine-trained rats (Fig.1v). We then assessed % silent synapses 6 hr after cue re-exposure, the time point at which the synapses re-silenced by cue re-exposure have normally re-matured (Fig. 1v). Infusion of either peptide did not alter the % silent synapses in saline-trained rats (Figs. 3c,f,S4b,d,e), suggesting that these peptides do not influence silent synapses at baseline. Cocaine-trained rats with NAcSh AGL exhibited low % silent synapses, which was increased by naspm, indicating the expected re-maturation of silent synapses (Figs. 3d,f,S4c,d,f). In contrast, TGL rats exhibited persistently high % silent synapses, and application of naspm did not further change this percentage (Fig.3e,f,S4g). Thus, preventing synaptic insertion of GluA1 AMPARs prevents re-maturation of the re-silenced synapses after cue re-exposure, and locks cocaine-generated synapses in the destabilized state.

Our subsequent results show that, when administered within the destabilization window, TGL also prevented weakened spines from re-maturation (Fig.3b). Specifically, infusion of TGL 2 hr after cue re-exposure did not change the densities of any spine subtypes in saline-trained rats (Fig.3g–k,S4h–j). However, after 45 days of withdrawal from cocaine, the cue re-exposure-induced upshift of thin spines and downshift of mushroom-like spines, which would otherwise return to the pre re-exposure levels 6 hr later (Fig.2), were maintained in TGL rats (Fig.3g–j). Thus, the spines that were weakened by cue re-exposure in cocaine-trained rats (Fig.2) were effectively locked in their weakened state by TGL-mediated blockade of GluA1 AMPAR trafficking. Consistently, the mean diameter of spine heads in cocaine-trained TGL rats was similar to saline-trained rats, and lower than cocaine-trained AGL rats (Fig.3l). Meanwhile, cocaine-trained rats with either AGL or TGL infusion

exhibited higher densities of total spines compared to saline-trained rats, and AGL did not prevent re-maturation of cue re-exposure-induced thin spines (Fig.3h–j). Furthermore, stubby spines were largely insensitive to TGL (Fig.3k).

If re-silencing and re-maturation of cocaine-generated synapses underlie the destabilization and reconsolidation of cocaine memories, preventing their re-maturation should disrupt reconsolidation and decrease the rats' responses to cocaine cues. To test this idea, we treated cocaine-trained rats using the same peptide procedure (Fig.3b), and measured cocaine seeking 6 hr after cue re-exposure, a time point at which cocaine seeking was robust in cocaine-trained rats with no peptide infusion (Fig.S5a–c). Infusion of either AGL or TGL did not affect operant responding in saline-trained rats (Fig.S5d,e,g,h), indicating minimal off-target effects of these peptides. However, cocaine-trained TGL rats exhibited decreased cocaine seeking compared to AGL rats when tested 6 hr after cue re-exposure, suggesting that preventing re-maturation of cocaine-generated silent synapses once they are re-silenced during the destabilization window compromises reconsolidation of cocaine-cue memories (Figs.3m,S5i). Note that during the 10-min cue re-exposure, AGL and TGL rats exhibited similar levels of cocaine seeking, indicating similar memory reactivation in these rats before peptide administration (Fig.S5f). Importantly, when peptides were infused 6 hr after cue re-exposure, a time point outside of the hypothesized destabilization window, cocaine-trained TGL rats exhibited similarly high levels of cocaine seeking as in cocaine-trained AGL rats, suggesting that once silent synapses have re-matured, cocaine memories become resistant to TGL manipulations (Figs.3n,S5f,j). These results reveal a causal link of the functional dynamics of cocaine-generated synapses to the destabilization and reconsolidation of cocaine memories.

Decreased Rac1 activity primes cue-induced synaptic re-silencing

To explore the molecular mechanisms that switch on and off silent synapse-mediated destabilization of cocaine memories, we focused on Rac1, a small GTPase, whose active forms are enriched in mature synapses to maintain synaptic stability through LIMK-cofilin-mediated regulation of actin cytoskeleton[30,31]. Using ELISA, we observed that after cue re-exposure on withdrawal day 45, levels of active Rac1 (Rac1-GTP) in the NAcSh were decreased transiently in cocaine-trained rats, and then returned to normal levels 6 hr later (Fig.4a). As controls, cue re-exposure did not affect levels of active Rac1 in saline-trained rats (Fig.4a).

The above results prompted us to test whether the decrease in active Rac1 destabilizes cocaine-generated synapses to allow their re-silencing after cue re-exposure (Fig.4b). We thus used a herpes simplex virus (HSV) vector to express a dominant negative form (dn) of Rac1, which interferes with the activity of endogenously active Rac1, in the NAcSh 45 days after cocaine self-administration. We then assessed silent synapses in HSV-infected MSNs ~12–16 hr after viral injection (Fig.4c,d). dnRac1 expression had no effect on basal % silent synapses in saline-trained rats (Figs.4e,h,S6a), indicating that dnRac1 expression alone does not generate silent synapses in the NAcSh of rats without cocaine experience. In contrast, silent synapses re-emerged in dnRac1-expresing NAcSh MSNs in cocaine-trained rats (Figs. 4f,h,S6b,c), to the levels similar to those restored in non-transduced MSNs by naspm (Figs.

4h,S6d). Additionally, application of naspm did not further affect the % silent synapses in dnRac1-expressing MSNs (Fig.4g,h), suggesting that the silent synapses observed after dnRac1 were the same set of cocaine-generated silent synapses. These effects of dnRac1 are not likely due to nonspecific effects of HSV transduction or protein overexpression since a control HSV (HSV-C450M), which expresses a mutant, nonfunctional form of Rac1, exerted no effect on silent synapses (Fig.S7).

While HSV expression of dnRac1 ensures sufficient Rac1 inhibition, it does not effectively capture the rapid temporal dynamics of synaptic re-silencing that naturally occurs following cue re-exposure. To manipulate dnRac1 in a temporally-controlled manner, we expressed a photoactivatable form of dnRac1 (pa-dnRac1), in which dnRac1 is fused with a photoreactive light oxygen voltage (LOV) domain, which prevents dnRac1 from interacting with its effectors[32, 33] (Fig.4i–k). Upon exposure to 473-nm laser, the LOV domain dissociates from dnRac1, allowing dnRac1 to bind to its effectors in a temporally-controlled manner (Fig.4k).

On withdrawal day 45, we injected HSV-pa-dnRac1 bilaterally into the rat NAcSh, and 12–16 hr later, inserted optical fibers into NAcSh through preinstalled guide cannulae (Fig.4i,j). We photo-stimulated NAcSh pa-dnRac1 for 10 min while rats were in their home cages, and assessed for silent synapses in transduced neurons immediately after. This manipulation did not affect the % silent synapses in saline-trained rats (Figs.4l,o,S6e), but increased the % silent synapses in cocaine-trained rats (Figs.4m,o,S6f). Furthermore, application of naspm did not additionally change this % (Fig.4n,o), again suggesting that silent synapses observed after dnRac1 stimulation were the same, cocaine-generated synapses. Taken together, a transient decrease in active Rac1 levels is sufficient to destabilize cocaine-generated synapses from the matured state for re-silencing.

We used cue-induced cocaine seeking as a final behavioral readout, which is presumably driven by several interwoven mechanisms and factors, including the memory intensity, memory reactivation efficacy, and intermediate steps of memories that drive the ongoing behaviors. To gain insight into which mechanisms involve silent synapses, we measured cocaine seeking 2 hr after cue re-exposure, when cocaine-generated synapses were in their re-silenced state. Cocaine-trained rats exhibited high levels of cocaine seeking at this time point (Figs.4p,S6g). This result dissociates the dynamics of silent synapses from the ongoing expression of cocaine seeking during the memory destabilization window. Indeed, similar dissociation is also observed in fear memories, in which the behavioral readout of fear memories remains at high levels during the destabilization window after memory reactivation[34]. Therefore, the state of NAcSh silent synapses does not determine the expression of cocaine seeking once the memories are reactivated. In contrast, when using pa-dnRac1 to manipulate the state of cocaine-generated synapses, we observed that re-silencing these synapses before, but not after, cue re-exposure-induced memory reactivation, reduced cocaine seeking (Figs.4q,S6j–p). Thus, the state of cocaine-generated NAcSh synapses may preferentially control the intensity of stored memories or memory reactivation processes, while once activated, the behavioral expression of these memories during the destabilization window is driven by other processes (Fig.4r).

High levels of active Rac1 stabilize synaptic state

We next tested whether maintaining high levels of active Rac1 prevents the re-silencing of cocaine-generated synapses in response to cue re-exposure. We expressed a constitutively active mutant (ca) of Rac1, which is locked within its active conformation[31]. 12–16 hr after intra-NAcSh injection of HSV-caRac1, saline- or cocaine-trained rats received cue re-exposure (on withdrawal day 45) and were assessed for silent synapses 10 min later (Fig.5a). Expression of caRac1 did not affect the % silent synapses in saline-trained rats with cue re-exposure (Figs.5b,e,S8a,c), but prevented cue re-exposure-induced re-emergence of silent synapses in cocaine-trained rats (Figs.5c,e,S8b–d). Application of naspm restored the high % silent synapses in caRac1-expressing MSNs (Figs.5d,e,S8e), indicating that cocaine-generated silent synapses were stabilized in their unsilenced, mature state. Thus, maintaining high levels of active Rac1 prevents the re-silencing of cocaine-generated synapses after memory retrieval.

To characterize Rac1's temporally dynamic regulation, we employed a photoactivatable form of caRac1 (HSV-paRac1[31]) (Fig.5f–h). On withdrawal day 45, we injected HSV-paRac1 bilaterally in the NAcSh, and 12–16 hr later, inserted optical fibers through preinstalled guide cannulae (Fig.5f,g). Stimulation of NAcSh paRac1 during cue re-exposure did not affect the % silent synapses in saline-trained rats (Figs.5i,l,S8f–h), but prevented the cue re-exposure-induced increase in the % silent synapses in cocaine-trained rats (Figs.5j,l, S8f–h). The low % silent synapses in these paRac1 MSNs was restored to high levels by application of naspm (Fig.5k,l), indicating that the cocaine-generated synapses were not eliminated but stabilized in the unsilenced state with CP-AMPARs when high levels of active Rac1 were maintained.

Our subsequent spine morphology results mirror the electrophysiological findings. Specifically, stimulation of paRac1 did not change the density of total spines in either saline- or cocaine-trained rats compared to non-transduced MSNs within the same rats (Figs. 5m,n,S8l–n). However, cue re-exposure-contingent paRac1 stimulation maintained the high density of mushroom-like spines and low density of thin spines in cocaine-trained rats during the subsequent destabilization window (Fig.5o,p), preventing the spine weakening process induced by cue re-exposure (Fig.2). Consistently, photostimulation stimulation also maintained the high mean spine head diameter of dendritic spines in paRac1-expressing MSNs, compared to non-transduced MSNs in the same cocaine-trained rats with cue re-exposure (Fig.5r). Note that paRac1 stimulation also slightly affected the spine densities and spine head diameter in saline-trained rats (Fig.5o–r), but these potentially nonspecific effects (~5%) are rather minimal and, in our view, do not confound the interpretation of our results from cocaine-trained rats.

PAK-LIMK-cofilin signaling serves as a key mechanistic pathway through which active Rac1 suppresses actin depolymerization and stabilizes synapses[30]. To test whether this pathway is utilized by paRac1 to prevent the re-silencing of cocaine-generated synapses following cue re-exposure, we infused a LIMK inhibitor (LIMKi) into the NAcSh ~20 min prior to photostimulation to disconnect the link between LIMK and Rac1 (Fig.5s). In cocaine-trained rats with vehicle infusion, paRac1 stimulation prevented the re-emergence of silent synapses after cue re-exposure (Figs.5t,v,S8i–k). However, paRac1 stimulation could

no longer prevent cue re-exposure-induced re-emergence of silent synapses in cocaine-trained rats given intra-NAcSh LIMKi infusion (Fig.5u,v). These results suggest that active Rac1 stabilizes cocaine-generated synapses through the LIMK-cofilin pathway-mediated regulation of actin skeleton.

Stabilizing cocaine-generated synapses in the weakened state

The above results show that, while a decrease in active Rac1 triggers dynamic changes (silencing) in the synaptic state of cocaine-trained rats, maintaining high levels of active Rac1 locks synapses in their current mature state despite cue re-exposure. We thus asked whether active Rac1 can also lock cocaine-generated synapses within the weakened state once they are re-silenced after cue re-exposure. We again used HSV-paRac1 to stimulate Rac1 activity in cocaine-trained rats but *2 hr* after cue re-exposure, when cocaine-generated synapses are re-silenced (Fig.6a,b), and assessed silent synapses 6 hr later, when cocaine-generated synapses normally return to a mature state. We observed that the % silent synapses was not affected in saline-trained rats (Figs.6c,f,S9a–c), but maintained at high levels in cocaine-trained rats (Figs.6d,f). In addition, the % silent synapses were not further increased upon naspm application (Fig.6e,f). Thus, after cocaine-generated synapses are re-silenced by cue re-exposure, a high level of Rac1 is capable of maintaining them in the silent state.

Following the same paRac1-cue procedures, MSNs with paRac1 stimulation exhibited similar density of total spines (Fig.6g,h,S9g–i), but lower densities of mushroom-like spines (Fig.6g,i) and higher densities of thin spines, compared to non-transduced MSNs from the same rats (Fig.6g,j). The concurrent downshift of mushroom-like and upshift of thin spines suggest that cocaine-generated synapses weakened by cue re-exposure were stabilized in the weakened state. This conclusion is further supported by observations of decreased mean spine head diameter in MSNs with paRac1 stimulation (Fig.6l). Meanwhile, paRac1 stimulation did not affect any dendritic spine subtypes in saline-trained rats (Fig.6g–k).

As for locking mature synapses, the PAK-LIMK-cofilin pathway is also essential for active Rac1 to lock cocaine-generated synapses within a silent, weakened state (Fig.6m). In cocaine-trained rats, intra-NAcSh infusion of LIMKi, but not vehicle, ~20 min prior to photostimulation prevented paRac1 from maintaining high levels of silent synapses beyond the 6 hr destabilization window (Figs.6n–p,S9d–f). Thus, the same cytoskeleton-regulating pathway is employed by active Rac1 to lock cocaine-generated synapses in their current state, regardless of whether they are in a silent or unsilenced state. It is worth noting that the PAK-LIMK-cofilin pathway in vivo likely responds to the fluctuations of active Rac1 levels in a highly dynamic and complicated manner. As such, intervention of this pathway with different timing may result in different synaptic consequences.

If the functional state of cocaine-generated synapses in the NAcSh dictates the strength or reactivation of cocaine memories as hypothesized, locking synapses in their mature and silent states should preserve and compromise the behavioral outputs of cocaine memories, respectively. To test this idea, we first stabilized cocaine-generated synapses in their mature state by stimulating paRac1 in cocaine-trained rats during cue re-exposure (Fig.5f), and measured cue-induced cocaine seeking 6 hr later (Fig.6q). Cocaine-trained rats that received

this paRac1 stimulation exhibited high cocaine seeking, comparable to control rats (with the same cocaine and photostimulation procedures, but expressing the control HSV-C450M) (Figs.6q,S10d,S11d–f,j–l). As an additional control, paRac1 stimulation also did not affect operant responding in saline-trained rats (Figs.S10a–c,S11a–c,g–i). In contrast, when we stabilized cocaine-generated synapses in their silent state by stimulating paRac1 2 hr after cue re-exposure (Fig.6a), cue-induced cocaine seeking was decreased, compared to C450M control rats when measured 6 hr after cue re-exposure (Figs.6r,S10h,S12d–f, j–l). This manipulation did not affect operant responding in saline-trained rats (Figs.S10e–g,S12a–c,g–i).

To examine whether this potential anti-relapse effect of paRac1 was due to long-term memory alteration, we tested another set of cocaine-trained rats with two paRac1 stimulations within the destabilization window (2 and 5 hr after cue re-exposure). These rats exhibited lower levels of cue-induced cocaine seeking compared to C450 control rats when measured >24 hr after cue re-exposure (Figs.6s,S10i,S13). Thus, stabilizing cocaine-generated synapses in a silent state through paRac1 undermines the intensity or reactivation of cocaine memories, leading to decreased cocaine seeking.

Discussion

The synaptic mechanisms underlying destabilization and reconsolidation of drug-associated memories remain largely elusive. Our current findings provide such a mechanism, in which the dynamic state of a specific population of synapses, initially generated by cocaine experience, controls the destabilization and reconsolidation of cocaine memories. We propose that these cocaine-generated synapses represent a discrete synaptic ensemble through which key aspects of cocaine-associated memories can be manipulated for therapeutic benefit.

Silent synapses regulate cocaine memories

Memories are not static. After formation and consolidation, stabilized memories can be destabilized again upon memory retrieval, followed by reconsolidation[4]. The destabilization not only allows for updating memories in response to changing outcomes, but also provides a therapeutic opportunity to weaken undesirable memories[7,35]. Although synapses are important memory-encoding substrates, how synapses operate to mediate these memory dynamics remains elusive. AMPAR-silent excitatory synapses are generated in the NAcSh when rats acquire cue-conditioned cocaine self-administration, and then mature over prolonged withdrawal as cue-induced cocaine seeking strengthens[16,18]. Here, we demonstrate that these synapses are re-silenced and weakened upon memory destabilization following memory reactivation, and then re-mature when the memory reconsolidates (Fig.1). When these synapses are held in the silent state after memory retrieval-induced re-silencing, reconsolidation is compromised, resulting in decreased cocaine seeking (Figs.3,6). These findings depict cocaine-generated silent synapses as key cellular substrates underlying the dynamic process of memory destabilization and reconsolidation. As such, cocaine memories, and possibly other memories as well, can be mechanistically manipulated through

specific underlying populations of synapses during the memory destabilization window, during which these synapses are naturally destabilized and primed for modification.

During the destabilization window, while cocaine-generated synapses are in a silent state, cue-induced cocaine seeking remains substantially elevated. However, when cocaine-generated synapses were silenced before memory reactivation, cue-induced cocaine seeking was decreased[16,18] (Figs.3,4,6). Thus, a dissociation between the functional state of cocaine-generated synapses and behavioral expression of cocaine memories emerges. We hypothesize that cocaine-generated synapses are key substrates for the storage or reactivation of cocaine memories; once the memories are reactivated, the behavioral expression is maintained by an independent set of mechanisms. This hypothesis explains high levels of cocaine seeking during the memory destabilization window in our current studies of cocaine memories, as well as in studies of fear memories[34]. This mechanistic dissociation is physiologically beneficial, as it allows for the memory-encoding substrates to be destabilized for modification without sacrificing the ongoing behavioral output.

Projections from limbic and paralimbic regions form heterogenous excitatory synapses onto NAc MSNs, regulating a wide range of emotional, motivational, and cognitive responses[36]. Drug addiction is expressed as alterations in selective, but not all, aspects of behavioral responses[2]. It is thus expected that, while cocaine memories can be encoded in many of these afferents, within an individual projection, only a select population of synapses contributes to cocaine memories[37]. Our present study randomly sampled silent synapses, presumably from all main NAc excitatory inputs that likely encompass many different aspects of cocaine memories. We have previously found that cocaine experience generates silent synapses in all NAc afferents that have been examined[16,17,38], and silent synapses in these distinct projections have different behavioral influences[17]. Therefore, silent synapses within individual projections may encode specific aspects of cocaine memories, while collectively these synapses encode broader, multifaceted cocaine memories. Sharing similar biophysical and biochemical properties, cocaine-generated synapses across different NAc afferents as a whole can be collectively manipulated to maximize therapeutic benefit.

Signaling substrates governing synaptic state

Once formed, synapses can be held in a highly stable state for a lifetime, or destabilized and eliminated during memory retrieval and reconsolidation[39]. The stability of synapses is finely controlled by signaling molecules, among which Rho family GTPases, particularly Rac1[31,40,41], control focal changes in activated synapses[42]. Following cocaine memory retrieval, the level of active Rac1 transiently decreases, and mimicking this decrease destabilizes cocaine-generated synapses (Fig.4). Conversely, increasing active Rac1 levels prevents the natural re-silencing of cocaine-generated synapses after memory retrieval (Fig. 5). These findings suggest that active Rac1 stabilizes synapses, while dynamic decreases in active Rac1 levels destabilize synapses for modification. Importantly, restoring high levels of active Rac1 during the destabilization window is also capable of stabilizing cocaine-generated synapses in their silent state (Fig.6), indicating that active Rac1 stabilizes synapses in their current state, irrespective of whether they are in a weakened or strengthened state. In this case, Rac1-based manipulations might be developed to turn on

and off the silent synapse-based memory destabilization window at intended time points beyond the classical 6-hr window for therapeutic need.

Our findings that Rac1 stabilizes the synaptic state are consistent with the general role of Rac1 in regulating synaptic scaffolds. Specifically, Rac1 activates the PAK-LIMK signaling pathway (Figs.5,6), which inhibits cofilin[30]. Cofilin regulates the actin cytoskeleton by two main mechanisms: actin severing, and increasing the off-rate of actin monomers, both favoring actin depolymerization[30]. However, actin severing also generates free barbed ends for elaboration and polymerization of actin, favoring actin polymerization[43]. Thus, the dynamic balance between these two processes determines how a change in Rac1-cofilin signaling affects the current synaptic state. In mature and stably functioning synapses, the level of active Rac1 is often persistently high[44], resulting in persistent inhibition of cofilin that prevents both actin depolymerization-mediated structural shrinkage and actin polymerization-mediated enlargement. Such a high stability of actin scaffolding and synaptic structure favors AMPARs to be maintained within the postsynaptic density (PSD)[30] and molecular trafficking to be confined within the synapse[45], promoting the functional stability of synapses. In contrast, a decrease in active Rac1 levels is required for synaptic changes, such as generation and potentiation of new synapses after cocaine experience, but maintaining high levels of active Rac1 prevents this synaptic remodeling[31]. Based on these results and analyses, we interpret the role of Rac1 after cocaine withdrawal such that a decrease in active Rac1 levels is a permissive step for CP-AMPAR internalization, while the CP-AMPAR internalization is driven by Rac1-independent mechanisms.

Complexities of cocaine memories

Cocaine-associated memories are complex and contain information related to unconditioned responses, conditioned stimuli, motivational attributes, and action, which involve diverse brain regions. These different memory components are not reactivated in isolation in our experimental setups as the rats are exposed to the cues and context, and allowed to respond operantly. Therefore, our results do not specify which specific components of cocaine memories are controlled by cocaine-generated synapses. However, significant clues exist. Specifically, previous results suggest that, rather than the CS-US reconsolidation of cocaine memories[46,47], the NAc may preferentially encode the motivational attributes and CS-action association components of memories[47, 48], leading to our speculation that NAc silent synapses are preferentially involved in the motivational and action-related aspects of cocaine memories.

When evaluating the translational potential of our current findings, boundary effects should be considered. While the training procedures used in the current study produce robust and persistent memories and 'incubated' drug seeking (Fig.1)[16–18] typically seen after extensive exposure to drugs[19,23], they do not adequately model the overtraining that occurs in human subjects with years of drug taking[49]. Overtraining can produce memories that are resistant to destabilization upon traditional memory reactivation[49]. Such boundary conditions may explain some discrepancies in the literature utilizing different training procedures and test memory performance at different time points after acquisition[46,47], since boundary conditions can be transient[50]. It is important for future studies to determine whether such

boundary conditions result from impaired re-silencing of cocaine-generated synapses and, importantly, whether NAc silent synapses remain as effective anti-relapse targets after cocaine overtraining.

Concluding remarks

Cocaine-generated silent synapses are sparsely distributed across several NAc afferents, but collectively form a unique synaptic population, whose dynamic changes control the encoding, destabilization and reconsolidation of cocaine memories. These synapses may represent a discrete synaptic engram, with which cocaine memories are stored, retrieved, and reconsolidated, and can be potentially targeted for clinical benefits.

Methods

Subjects:

Male Sprague-Dawley rats (postnatal day 35–40 with 130–150 g body weight upon arrival) (Charles River) were used in all experiments. Rats were singly housed on a 12-hr light/dark cycle (light on/off at 7:00 am/pm) with food and water available *ad libitum*. Rats were allowed to habituate to their housing cages for ~1 week before the catheter surgery. All rats were used in accordance with protocols approved by the Institutional Care and Use Committees at the University of Pittsburgh and Icahn School of Medicine at Mount Sinai.

Catheter Implantation:

Self-administration surgery was performed as described previously[16, 51]. Briefly, a silastic catheter was inserted into the right jugular vein by 2.5 cm, and the distal end was led subcutaneously to the back between the scapulae. Catheters were constructed of silastic tubing (length, 10 cm; inner diameter, 0.020 in; outer diameter, 0.037 in) and connected to a commercially available Vascular Access Button (Instech). Rats were allowed to recover 3–5 day after surgery. During the recovery period, the catheter was flushed daily with 1 ml/kg heparin (10 U/ml) and gentamicin antibiotics (5 mg/ml) in sterile saline to minimize potential infection and catheter occlusion.

Self-administration apparatus:

Behavioral experiments were conducted in operant-conditioning chambers enclosed within sound-attenuating cabinets (Med Associates). Each chamber ($29.53 \times 24.84 \times 18.67$ cm) contains an active and an inactive nose poke hole, a food dispenser, a conditioned stimulus (CS) light in each nose poke hole, and a house light. No food or water was provided in the chamber during the training or testing sessions.

Intravenous cocaine self-administration training:

Cocaine self-administration training began ~5 days after surgery. On day 1, rats were placed in self-administration chambers for an overnight training session on a fixed ratio (FR) 1 reinforcement schedule. Nose poking in the active hole resulted in a cocaine infusion (0.75 mg/kg over 3–6 sec) and illumination of the CS light inside the nose poke hole as well as the house light. The CS light remained on for 6 sec, whereas the house light was illuminated for

20 sec, during which active nose pokes were counted but resulted in no cocaine infusions. After the 20-sec timeout period, the house light was turned off, and the next nose poke in the active hole resulted in a cocaine infusion. Nose pokes in the inactive hole had no reinforced consequences but were recorded. Rats first underwent one overnight training session (~12-hr) to facilitate acquisition. Only rats that received at least 80 cocaine infusions during the overnight session were allowed to receive the 5-day cocaine self-administration regimen (<2% of rats failed to meet this criteria). Same or similar self-administration procedures/ standards were used in our previous studies[16, 18, 51]. On the fifth day of training, rats were placed back into their home cages and remained there during subsequent withdrawal days. Cocaine-trained rats that failed to meet self-administration criteria (15 infusions/session, 70% active to inactive nose poke response ratio) were excluded from further experimentation and analysis. Note that rats with high inactive nose pokes relative to active were excluded as the inactive nose poke responding likely reflected unconditioned motor-stimulating effects (e.g., stereotypic biting of nose poke hole) rather than learned operant responses.

Withdrawal phase:

Rats were returned to their home cages after each cocaine self-administration session. After the 5-day procedure, the rats were singly housed in their home cages for drug withdrawal, with food and water available *ad libitum*. Withdrawal day 1 was operationally defined as 20–26 hr after the last session of cocaine self-administration. Withdrawal day 45 was operationally defined as 40–48 days after the last session of cocaine self-administration.

Memory retrieval:

Cue-induced memory retrieval sessions were performed in the same manner as the cue-induced cocaine seeking procedure as detailed below, except that the sessions lasted for 10–15 min.

Cue-induced cocaine seeking:

Cue-induced cocaine seeking was assessed in an extinction test (1 hr) conducted after 1-day or 45-day withdrawal from cocaine self-administration. During the extinction test session, active nose pokes resulted in contingent deliveries of the CS light cues but not cocaine. The number of nose pokes to the active holes was used to quantify cue-induced cocaine seeking, and the number of nose pokes to the inactive holes was used as controls.

GluA1 peptide:

The peptide TGL (SSGMPLGATGL) was used to interfere with GluA1 subunit-containing AMPAR trafficking. A similar peptide AGL (SSGMPLGAAGL) was used as the control for TGL. AGL has a single different amino acid that prevents the peptide from interfering with GluA1[27]. These two peptides were conjugated with a trans-activating transcriptional activator (TAT) sequence (GRKKRRQRRRPQ) to facilitate intracellular delivery, resulting in TAT-pep1-TGL (GRKKRRQRRRPQSSGMPLGATGL) and TAT-pep1-AGL (GRKKRRQRRRPQSSGMPLGAAGL). TAT-TGL and TAT-AGL were custom-made from GenScript (Piscataway, NJ).

Peptide and LIMKi injections:

For peptide injections, on withdrawal day 35, rats (350–400 g) were bilaterally implanted with guide cannulae (Plastics One) targeting the NAcSh (in mm: AP, +1.60; ML, ±1.00; DV, −6.80). On withdrawal day 45, at the specified time point (e.g., 2 or 6 hr) after cue re-exposure (see below), rats were lightly anesthetized and peptide (30 μM) was infused through 32-gauge needles extending 1 mm below the cannula into the NAcSh (in mm: AP, +1.60; ML, ±1.00; DV, −7.80). For electrophysiological experiments, 1 μl/side (30 pmol/side) was injected to maximize peptide spread throughout the recording area. For behavioral experiments, 0.5 μl/side (15 pmol/side) was injected to ensure the NAcSh-confined effects. Peptide was infused at a rate of 200 nl/min, and the infusing needle was left in place for 5 min to minimize backflow. Based on injections of EvansBlue dye, 1-μl infusions diffused throughout the NAcSh and into the NAc core, and 0.5-μl infusions were confined within the NAcSh. In addition, previous studies utilizing similar peptides and TAT sequences confirm that the vast majority of neurons within the infusion area take up the peptide[52]. For electrophysiology experiments, in order to ensure recordings were made from MSNs within the infusion area, all recordings were made within the ~200-μm radius from the center of the injection site, an area well within the boundaries covered by the infusion. The injection sites of each rat for behavioral tests were assessed by injecting 0.5-μl EvansBlue dye using the same approach as for peptide injections. Rats were subsequently decapitated under deep isoflurane anesthesia and coronal slices (300-μm thick) containing NAc were prepared on a VT1200S vibratome (Leica) in PBS. Localizations of EvansBlue dye were determined visually and recorded. Rats with inaccurate injections were excluded from data analysis.

To manipulate the PAK-LIMK-cofilin pathway *in vivo*, we infused CRT0105950 (Tocris), a highly selective LIMK1/2 inhibitor (LIMKi)[53]. LIMKi was dissolved in 1% DMSO and 0.1 M Dulbecco's sterile phosphate buffered saline (PBS). 1% DMSO and 0.1 M Dulbecco's sterile PBS were used as the vehicle control. Infusion of the LIMKi to the NAcSh was performed as described above. Briefly, LIMKi at 10 μM (1 μl/side), a dose shown to sufficiently inhibit LIMK with minimal negative effects on cell viability[53], was infused into the NAcSh through a preinstalled cannula at a rate of 200 nl/min. Similar to peptide experiments, all electrophysiology recordings were performed within the 200 mm-radius of the injection center.

Viral vectors and delivery:

We used the bicistronic p1005+ HSV vector to express dnRac1, caRac1, Rac1-C450M (control), pa-dnRac1, and paRac1 combined with GFP or mCherry, as described previously[31, 32]. These HSVs were prepared using the same methods described previously[31, 54, 55]. Prior work shows that HSVs infect neurons only, and in the NAc, the vast majority of HSV-infected neurons are MSNs[56]. In our recordings, we came across very few transduced inhibitory interneurons (~10 throughout the entire study) and no transduced cholinergic interneurons. Thus, effects mediated by HSV-mediated transduction are most attributable to MSNs.

Due to the rapid and transient HSV-mediated expression, rats were bilaterally implanted with guide cannulae (Plastics One) targeting the NAcSh on withdrawal day 35, as described

above. Rats were injected with HSVs 12–16 hr before electrophysiological or behavioral experiments on withdrawal day 45. During injection, rats were lightly anesthetized and HSV (1 μl/side) was bilaterally infused (100 nl/min) through 32-gauge needles extending 1 mm below the cannulae into the NAc shell (in mm: AP, +1.60; ML, ±1.00; DV, −7.80). Infusing needles were left in place for 10 min following injection to prevent backflow and allow for sufficient diffusion of HSV vectors away from the injection site. This approach minimized potential behavioral disturbance following acute intracranial surgeries and allowed for the insertion of optic fibers for the photoactivation experiments (see below).

For electrophysiology experiments, viral injections and expression were visually verified in brain slices prepared for recording, while for behavioral experiments, immunohistochemistry and confocal microscopy (see below) were used for verification. Rats with inaccurate injections or weak viral expression were excluded from data analysis.

Photoactivation of paRac1:

The activity of paRac1 is sharply increased following photostimulation, and then decays exponentially with a $T_{1/2}$ = ~10 sec at room temperature [32]. The decay kinetics are likely faster *in vivo*. We used a stimulation protocol comprised of the 473-nm laser pulses at the frequency of 10 Hz, pulse duration of 0.5-ms, and laser intensity of 10 mW/mm². Laser was generated and controlled by a 473-nm blue laser diode (IkeCool, CA), and the pulse patterns were generated through a waveform isolator (A.M.P.I.). The photostimulation protocol was delivered for 10 min to match the duration of cue re-exposure. Stimulation parameters in this protocol have been verified to introduce minimal tissue damage in behaving rats in our previous studies[57], and was used in all photoactivation experiments presented in this manuscript.

For in vivo photostimulation experiments, rats were bilaterally implanted with guide cannulae (Plastics One) targeting the NAc Shell (in mm: AP, +1.60; ML, ±1.00; DV, −6.00) on withdrawal day 35. For rats receiving photostimulation on withdrawal day 45, the rats were slightly restrained and two 200-μm core optic fibers were bilaterally inserted through the cannulae. The length of the optical fiber was adjusted such that the tip would rest ~300 μm dorsal to the viral injection site (in mm: AP, +1.60; ML, ±1.00; DV, −7.50). Immediately after the optic fiber was secured, the rat was placed back into their home cage (pa-dnRac1 in Fig. 4 and 2hr post paRac1 in Fig. 6) or in the operant chamber (paRac1 during re-exposure in Fig. 5), with the fiber attached to a tether system to allow rats for free movement during photostimulation. After the stimulation session, the optic fibers were removed and the rat was placed back into its home cage. For behavioral experiments testing the effects of paRac1 activation 24 hr after cue re-exposure, a second photostimulation session 5 hr after cue re-exposure was performed to extend the duration of Rac1 activation within the destabilization window.

Rac1 assay:

At specified time points, the rats were sacrificed by decapitation, and the brain was quickly removed and snap frozen in 2-Methylbutane (Sigma Aldrich, St. Louis, MO) for 1 min. Using a brain matrix, 2-mm thick brain slices were prepared and tissue punches containing

the NAc were extracted. The punched tissue was homogenized in lysis buffer (4ºC) and then centrifuged at 14000 g for 2 min at 4ºC. The supernatant was collected and snap frozen. Lysate was stored at –80ºC. Rac1-GTP was quantified with the Rac1 G-LISA Activation Assay (Absorbance Based) (Cytoskeleton, Denver) according to the manufacture instructions. Rac1-GTP levels were then assessed by the absorbance of each sample at 490 nm.

Preparation of acute brain slices:

Rats were decapitated following isoflurane anesthesia. For NAc containing slices, coronal slices (250-μm thick) containing the NAc were prepared on a VT1200S vibratome (Leica) in 4°C cutting solution containing (in mM): 135 N-methyl-d-glutamine, 1 KCl, 1.2 KH_2PO_4, 0.5 $CaCl_2$, 1.5 $MgCl_2$, 20 choline-HCO_3, and 11 glucose, saturated with 95%O_2/5%CO_2, pH adjusted to 7.4 with HCl. Osmolality was adjusted to 305. For hippocampal recordings, transverse slices (400-μm thick) containing the ventral hippocampus were prepared on a VT1200S vibratome (Leica) in 4°C cutting solution. A small cut was made in the CA3 region to prevent epileptic activities in the CA1 region. Slices were incubated in the artificial cerebrospinal fluid (aCSF) containing (in mM): 119 NaCl, 2.5 KCl, 2.5 $CaCl_2$, 1.3 $MgCl_2$, 1 NaH_2PO_4, 26.2 $NaHCO_3$, and 11 glucose with the osmolality adjusted to 280–290. Slices were placed in the aCSF saturated with 95% O_2 / 5% CO_2 at 37°C for 30 min and then held at 20–22°C for at least 30 min before experimentation.

Electrophysiological recordings:

Extracellular field recordings: All field recordings were made within the CA1 region of the hippocampus. Prior to recordings, hippocampal slices were incubated with 200 μM TGL or 200 μM AGL for >1 h. During recordings, slices were superfused with high divalent aCSF, containing the same ingredients as the holding aCSF except that 4 mM $CaCl_2$ and $MgCl_2$ were used to replace 2.5 mM $CaCl_2$ and 1.3 mM $MgCl_2$. Recordings were made by placing a recording electrode filled with 2 M NaCl in the stratum radiatum of the CA1. Schaffer collaterals originating from the CA3 were stimulated with by a constant-current isolated stimulator (Digitimer), using a monopolar electrode (glass pipette filled with aCSF). Synaptic currents were recorded with a MultiClamp 700B amplifier, filtered at 2.6–3 kHz, amplified five times, and then digitized at 20 kHz. A high frequency stimulation (HFS: two 1-sec trains at 100 Hz with a 20-sec interval, 1.5 times of the test current intensity) was used to induce LTP. In experiments involving inhibition of NMDARs, 50 μM APV was included in the bath.

Whole-cell recordings: All recordings were made from MSNs located in the medial NAcSh. During recordings, slices were superfused with aCSF, heated to 30–32°C by passing the solution through a feedback-controlled in-line heater (Warner) before entering the recording chamber. To measure minimal stimulation-evoked responses, electrodes (2–5 MΩ) were filled with a cesium-based internal solution (in mM: 135 $CsMeSO_3$, 5 CsCl, 5 TEA-Cl, 0.4 EGTA (Cs), 20 HEPES, 2.5 Mg-ATP, 0.25 Na-GTP, 1 QX-314 (Br), pH 7.3). Picrotoxin (0.1 mM) was included in the aCSF during all recordings to inhibit $GABA_A$ receptor–mediated currents. Presynaptic afferents were stimulated by a constant-current isolated stimulator (Digitimer), using a monopolar electrode (glass pipette filled with aCSF). Series

resistance was typically 7–20 MΩ, uncompensated, and monitored continuously during recording. Cells with a change in series resistance >20% were excluded from data analysis. Synaptic currents were recorded with a MultiClamp 700B amplifier, filtered at 2.6–3 kHz, amplified five times, and digitized at 20 kHz.

Detection of GluN2B-NMDAR currents: To measure NMDAR-mediated EPSCs, NBQX (5 μm) and picrotoxin (0.1 mM) were included in the bath. Recorded neurons were held at –40 mV to partially relive Mg^{2+}-mediated blockage of NMDARs. Following a 7-min baseline recording, the bath that additionally contained the GluN2B-selective antagonist Ro256981 (200 nM) was switched in. NMDAR EPSCs were continuously recorded as the new bath perfused the slice, but only EPSCs after 8 min were included for data analysis to allow diffusion of Ro256981 into the slice and this use-dependent antagonist to operate. After 10 min of recording, a bath containing APV (50 μM) instead of Ro256981 was switched in to inhibit all NMDARs, which verified that recorded EPSCs were mediated by NMDARs.

Detection of CP-AMPARs: To isolate AMPAR-mediated EPSCs, picrotoxin (0.1 mM) and APV (50 μM) were included in the bath. To properly assess the rectification of AMPAR EPSCs, spermine (0.1 mM) was freshly added to the internal solution. AMPAR EPSCs were evoked at progressively depolarized holding potentials (–70 mV to +50 mV with a 10-mV increment) to generate an *I-V* curve. Twelve responses were recorded at each holding potential and averaged. The rectification index was calculated by comparing the peak amplitude at +50 mV to –70 mV after correction for the reversal potential with the following equation:

$$\text{RI} = \left(I_{+50} / \left(50 - E_R\right)\right) / \left(I_{-70} / \left(-70 - E_R\right)\right)$$

where *I* is the peak amplitude at either +50 mV or –70 mV, and E_R is the reversal potential of AMPAR EPSCs, which was measured manually for each recorded neuron.

Silent synapse recordings and analysis: NAcSh MSNs were randomly selected for recording. The minimal stimulation assay was performed as previously described[12, 14–16, 18]. After obtaining small (~50 pA) EPSCs at –70 mV, the stimulation intensity was reduced in small increments to the point that failures versus successes of synaptically evoked events (EPSCs) could be clearly distinguished. The stimulation intensity and frequency were then kept constant for the rest of the experiment. The amplitude of both AMPAR and NMDAR ESPCs resulting from single vesicular release is relatively large in NAcSh MSNs (e.g., ~15 pA for AMPAR mEPSCs at –70 mV), which facilitates the judgment of successes versus failures. For each cell, 50–100 traces were recorded at –70 mV, and 50–100 traces were recorded at +50 mV. Recordings were then repeated at –70 mV and +50 mV for another round or two. Only cells with relatively constant failure rates (changes <15%) between rounds were used to assess % silent synapses. We visually detected failures versus successes at each holding potential over 50–100 trials to calculate the failure rate, as described previously[12, 16, 17]. We performed this analysis in a blind manner such that a small number of ambiguous responses were categorized in a fully unbiased way.

To quantify % silent synapses, we made two theoretical assumptions: 1) the presynaptic release sites are independent, and 2) release probability across all synapses, including silent synapses, is identical. Thus, % silent synapses was calculated using the equation: $1 - \ln(F_{-70})/\ln(F_{+50})$, in which F_{-70} was the failure rate at -70 mV and F_{+50} was the failure rate at $+50$ mV, as rationalized previously[15]. Note that in this equation, the failure rate is the only variable that determine the % silent synapses. The amplitudes of EPSCs are used to present failures or successes, but do not have analytical value. In the cases in which these two theoretical assumptions are not true, the above equation was still used, as the results were still valid in predicting the changes of silent synapses qualitatively as previously rationalized[17, 58]. The amplitude of an EPSC was determined as the mean value of the EPSC over a 1-ms time window around the peak, which was typically 3–4 ms after the stimulation artifact. To assess the % silent synapses, only the rates of failures versus successes, not the absolute values of the amplitudes, were used. At +50 mV, successful synaptic responses were conceivably mediated by both AMPARs and NMDARs, and inhibiting AMPARs by NBQX (5 μM) modestly reduces the amplitudes of EPSCs[20]. Despite the effects of NBQX on the amplitudes, the failure rate of synaptic responses at +50 mV was not altered during AMPAR inhibition[20]. Thus, in the minimal stimulation assay assessing the % silent synapses, the results will not be affected whether the synaptic responses +50 mV are mediated by NMDARs alone or by both AMPARs and NMDARs.

Immunohistochemistry and confocal microscopy:

One to four days after behavioral testing, when HSV expression remains readily detectable, rats were transcardially perfused with 0.1 M sodium phosphate buffer (PB), followed by 4% paraformaldehyde (PFA, wt/wt) in 0.1 M PB. Brains were removed and postfixed in 4% PFA overnight at 4ºC. Following postfix, whole brains were stored in 30% sucrose in PB with 0.1% sodium azide at 4ºC until sectioning. Coronal sections (100-μm thick) containing the NAc were then prepared on a VT1200S vibratome (Leica) in 0.1 M phosphate buffered saline (PBS) and then stored in cryoprotectant (30% sucrose, 30% ethelyne glycol, in PB) at −20ºC until staining.

Immunohistochemistry was performed as previously described[59]. Briefly, floating sections were washed in PBS 3 × 5 min and then permeablized with 0.1% Triton X-100 in PBS for 15 min. Sections were then washed 3 × 5 min in PBS and blocked with 5% normal donkey serum in PBS for 2 hr. Sections were next incubated overnight at 4ºC with a primary antibody against GFP (1:1000, monoclonal mouse anti-GFP; Abcam). Sections were subsequently washed 3 × 5 min in PBS and incubated for 2 hr at room temperature with a secondary antibody (1:500, ALEXA 488 donkey anti-mouse; Abcam). Sections were washed again 3 × 5 min in PBS before they were mounted in ProLong Gold Antifade with DAPI (Molecular Probes).

Sections were imaged and captured with a Leica TCS SP5 confocal microscope equipped with Leica Application Suite software (Leica microsystems). Slices were imaged with a 5x or 10x air objective and the entire slice was captured using automated tile scanning and image stitching functions. From these images, viral expression and localization could be determined. All representative images were captured with a 10x air objective. In addition,

high magnification images of transduced neurons were captured using a 40x oil immersion objective to verify viral expression in intact neurons.

Dendritic spine labeling and imaging:

To visualize dendritic spines, MSNs were filled with Alexa 594 dye using single-cell microinjections, and the labeled dendritic spines were quantified as described previously[60, 61]. Briefly, the rats were transcardially perfused with ice cold 1% PFA in 0.1 M PB, followed by 4% PFA and 0.125% glutaraldehyde in 0.1 M PB. Brains were removed and postfixed in 4% PFA and 0.125% glutaraldehyde in 0.1 M PB for 12–14 hr at 4ºC. Following postfix, the brains were transferred into 0.1 M PBS and sectioned into 250-μm thick slices using a VT1200S vibratome (Leica). Cells were filled shortly after slicing (within 4 hr). Cells within the NAcSh were impaled with a fine micropipette containing 5 mM Alexa 594 hydrazide (Invitrogen) and injected with 1–10 nA of negative current until dendrites and spines were filled. Based on the presence of GFP signals, transduced and non-transduced cells were visually targeted and filled in the same rat. After filling, the slices were mounted in ProLong Gold Antifade (Molecular Probes) on slides for imaging. 240-μm thick spacers were placed along the edge of the slide before mounting to avoid compression of the slices by the overlying coverslip and prevent deformation of spine morphologies.

Images were captured with a Leica TCS SP5 confocal microscope equipped with Leica Application Suite software (Leica). Individually filled neurons were visualized with a 63x oil immersion objective for final verification of their neuronal types (e.g., MSNs vs. interneurons). Individual dendritic segments were focused on and scanned at 0.69-μm intervals along the z-axis to obtain a z-stack. After captured, all images were deconvolved within the Leica Application Suite software. Analyses were performed on two-dimensional projection images using ImageJ (NIH). Secondary dendrites were sampled and analyzed due to their significant cellular and behavioral correlates[20, 62]. For each neuron, 1–4 (2.1 average) dendritic segments of ~20 μm in length were analyzed. For each group, 4–8 cells per rat were analyzed. For experiments examining the effects of paRac1 stimulation 4–8 non-transduced and 4–8 transduced cells were analyzed and compared from the same rat. Similar to our previous studies, we operationally divided spines into 3 categories[13, 20]: i) mushroom-like spines were dendritic protrusions with a head diameter >0.5 μm or >2x than the spine neck diameter; ii) stubby spines were dendritic protrusions with no discernable head and a length of   0.5 μm; iii) thin/filopodia-like spines were dendritic protrusions with a length of > 0.5 μm and head diameter < 0.5 μm or no discernable head. During counting of dendritic spines, spine head diameters were also measured for analysis.

Statistics:

All results are shown as mean ± s.e.m. All experiments were replicated in 3–16 rats. All data collection was randomized. All data were assumed to be normally distributed, but this was not formally tested. No statistical methods were used to pre-determine sample sizes, but our sample sizes are similar to those reported in previous publications[16–18]. All data were analyzed offline and investigators were blinded to experimental conditions during the analyses.

A total of 1034 rats were used for this study, among which 394 were excluded from the final data analysis and interpretation due to the following reasons: 1) 67 rats were excluded because of health issues after surgeries (e.g., >20% drop in body weight); 2) 272 were excluded because of the catheter failure, or failure in reaching the self-administration criteria; 3) 55 were excluded due to off-target stereotaxic injections or poor viral expression.

Repeated experiments for the same group were pooled together for statistical analysis. Sample sizes were based on our previous studies performing similar experiments[16, 18, 20]. For electrophysiology and dendritic spine experiments, the sample sizes are presented as n/m, where n = number of cells and m = number of rats. For behavioral experiments, the sample sizes are presented as n, which is the number of rats. Animal-based statistics were used for all data analyses, except for fEPSP electrophysiology experiments, in which n = number of recordings (Fig. S4a). For electrophysiological experiments, we averaged the values of all the cells from each rat to obtain an animal-based mean value for statistical analysis[16, 18, 20]. For dendritic spine experiments, we averaged individual dendritic segment values from each cell to obtain a cell-based value, and then averaged cell-based values from each rat to obtain animal-based values for statistical analysis[60, 61]. Normal distribution was assumed for all statistics, but not formally tested. Statistical significance was assessed using unpaired t-tests, one-way ANOVA, or repeated measures two-way ANOVA, as specified in the related text. Two-tailed tests were performed for analyses. Statistical significance was set at $p < 0.05$ for all experiments. Statistical analyses were performed in GraphPad Prism (v8). All main statistical results are presented in the main text, and additional statistical results are provided in Supplemental Table 1. Detailed experimental approaches, codes, and reagents are presented in the Life Sciences Reporting Summary section.

Supplementary Material

Refer to Web version on PubMed Central for supplementary material.

Acknowledgements:

References

1. Hyman SE, Malenka RC & Nestler EJ Neural mechanisms of addiction: the role of reward-related learning and memory. Annual review of neuroscience 29, 565–598 (2006).

2. Wolf ME Synaptic mechanisms underlying persistent cocaine craving. Nature Reviews Neuroscience 17, 351–365 (2016). [PubMed: 27150400]

3. Nader K. & Hardt O. A single standard for memory: the case for reconsolidation. Nat Rev Neurosci 10, 224–234 (2009). [PubMed: 19229241]

4. Tronson NC & Taylor JR Molecular mechanisms of memory reconsolidation. Nature Reviews Neuroscience 8, 262–275 (2007). [PubMed: 17342174]

5. Lee JLC, Di Ciano P, Thomas KL & Everitt BJ Disrupting reconsolidation of drug memories reduces cocaine-seeking behavior. Neuron 47, 795–801 (2005). [PubMed: 16157275]

6. Miller CA & Marshall JF Molecular substrates for retrieval and reconsolidation of cocaine-associated contextual memory. Neuron 47, 873–884 (2005). [PubMed: 16157281]

7. Torregrossa MM & Taylor JR Neuroscience of learning and memory for addiction medicine: from habit formation to memory reconsolidation. Prog Brain Res 223, 91–113 (2016). [PubMed: 26806773]

8. Jobes ML, et al. Effects of Prereactivation Propranolol on Cocaine Craving Elicited by Imagery Script/Cue Sets in Opioid-dependent Polydrug Users: A Randomized Study. J Addict Med 9, 491–498 (2015). [PubMed: 26501788]

9. Lonergan M, et al. Reactivating addiction-related memories under propranolol to reduce craving: A pilot randomized controlled trial. J Behav Ther Exp Psychiatry 50, 245–249 (2016). [PubMed: 26454715]

10. Dunbar AB & Taylor JR Reconsolidation and psychopathology: Moving towards reconsolidation-based treatments. Neurobiology of Learning and Memory 142, 162–171 (2017). [PubMed: 27838441]

11. Dong Y. & Nestler EJ The neural rejuvenation hypothesis of cocaine addiction. Trends in pharmacological sciences 35, 374–383 (2014). [PubMed: 24958329]

12. Huang YH, et al. In vivo cocaine experience generates silent synapses. Neuron 63, 40–47 (2009). [PubMed: 19607791]

13. Brown TE, et al. A silent synapse-based mechanism for cocaine-induced locomotor sensitization. J Neurosci 31, 8163–8174 (2011). [PubMed: 21632938]

14. Isaac JT, Nicoll RA & Malenka RC Evidence for silent synapses: implications for the expression of LTP. Neuron 15, 427–434 (1995). [PubMed: 7646894]

15. Liao D, Hessler NA & Malinow R. Activation of postsynaptically silent synapses during pairing-induced LTP in CA1 region of hippocampal slice. Nature 375, 400–404 (1995). [PubMed: 7760933]

16. Lee BR, et al. Maturation of silent synapses in amygdala-accumbens projection contributes to incubation of cocaine craving. Nature Neuroscience 16, 1644–1651 (2013). [PubMed: 24077564]

17. Ma Y-Y, et al. Bidirectional modulation of incubation of cocaine craving by silent synapse-based remodeling of prefrontal cortex to accumbens projections. Neuron 83, 1453–1467 (2014). [PubMed: 25199705]

18. Ma Y-Y, et al. Re-silencing of silent synapses unmasks anti-relapse effects of environmental enrichment. Proceedings of the National Academy of Sciences of the United States of America 113, 5089–5094 (2016). [PubMed: 27091967]

19. Grimm JW, Hope BT, Wise RA & Shaham Y. Neuroadaptation. Incubation of cocaine craving after withdrawal. Nature 412, 141–142 (2001). [PubMed: 11449260]

20. Graziane NM, et al. Opposing mechanisms mediate morphine- and cocaine-induced generation of silent synapses. Nature Neuroscience 19, 915–925 (2016). [PubMed: 27239940]

21. Hanse E, Seth H. & Riebe I. AMPA-silent synapses in brain development and pathology. Nature Reviews Neuroscience 14, 839–850 (2013). [PubMed: 24201185]

22. Cull-Candy S, Kelly L. & Farrant M. Regulation of Ca2+-permeable AMPA receptors: synaptic plasticity and beyond. Current Opinion in Neurobiology 16, 288–297 (2006). [PubMed: 16713244]

23. Conrad KL, et al. Formation of accumbens GluR2-lacking AMPA receptors mediates incubation of cocaine craving. Nature 454, 118–121 (2008). [PubMed: 18500330]

24. Nader K, Schafe GE & LeDoux JE Fear memories require protein synthesis in the amygdala for reconsolidation after retrieval. Nature 406, 722–726 (2000). [PubMed: 10963596]

25. Holtmaat A. & Svoboda K. Experience-dependent structural synaptic plasticity in the mammalian brain. Nature Reviews Neuroscience 10, 647–658 (2009). [PubMed: 19693029]

26. Matsuzaki M, et al. Dendritic spine geometry is critical for AMPA receptor expression in hippocampal CA1 pyramidal neurons. Nature Neuroscience 4, 1086–1092 (2001). [PubMed: 11687814]

27. Lin MT, et al. Coupled Activity-Dependent Trafficking of Synaptic SK2 Channels and AMPA Receptors. The Journal of neuroscience : the official journal of the Society for Neuroscience 30, 11726–11734 (2010). [PubMed: 20810893]

28. Hayashi Y, et al. Driving AMPA receptors into synapses by LTP and CaMKII: requirement for GluR1 and PDZ domain interaction. Science 287, 2262–2267 (2000). [PubMed: 10731148]

29. Zhou Z, et al. The C-terminal tails of endogenous GluA1 and GluA2 differentially contribute to hippocampal synaptic plasticity and learning. Nature Neuroscience, 1–19 (2017). [PubMed: 29238082]

30. Cingolani LA & Goda Y. Actin in action: the interplay between the actin cytoskeleton and synaptic efficacy. Nature Reviews Neuroscience 9, 344–356 (2008). [PubMed: 18425089]

31. Dietz DM, et al. Rac1 is essential in cocaine-induced structural plasticity of nucleus accumbens neurons. Nature Neuroscience 15, 891–896 (2012). [PubMed: 22522400]

32. Wu YI, et al. A genetically encoded photoactivatable Rac controls the motility of living cells. Nature 461, 104–108 (2009). [PubMed: 19693014]

33. Wang X, He L, Wu YI, Hahn KM & Montell DJ Light-mediated activation reveals a key role for Rac in collective guidance of cell movement in vivo. Nature Neuroscience 12, 591–597 (2010).

34. Monfils M-H, Cowansage KK, Klann E. & LeDoux JE Extinction-reconsolidation boundaries: key to persistent attenuation of fear memories. Science 324, 951–955 (2009). [PubMed: 19342552]

35. Lee JLC Memory reconsolidation mediates the strengthening of memories by additional learning. Nature Neuroscience 11, 1264–1266 (2008). [PubMed: 18849987]

36. Sesack SR & Grace AA Cortico-Basal Ganglia reward network: microcircuitry. Neuropsychopharmacology 35, 27–47 (2010). [PubMed: 19675534]

37. Cruz FC, et al. New technologies for examining the role of neuronal ensembles in drug addiction and fear. Nature Reviews Neuroscience 14, 743–754 (2013). [PubMed: 24088811]

38. Neumann PA, et al. Cocaine-Induced Synaptic Alterations in Thalamus to Nucleus Accumbens Projection. Neuropsychopharmacology 41, 2399–2410 (2016). [PubMed: 27074816]

39. Yang G, Pan F. & Gan W-B Stably maintained dendritic spines are associated with lifelong memories Nature 462, 920–924 (2009). [PubMed: 19946265]

40. Liao Z, et al. Fear Conditioning Downregulates Rac1 Activity in the Basolateral Amygdala Astrocytes to Facilitate the Formation of Fear Memory. Front Mol Neurosci 10, 396 (2017). [PubMed: 29230165]

41. Das A, Dines M, Alapin JM & Lamprecht R. Affecting long-term fear memory formation through optical control of Rac1 GTPase and PAK activity in lateral amygdala. Scientific Reports, 1–9 (2017). [PubMed: 28127051]

42. Nishiyama J. & Yasuda R. Biochemical Computation for Spine Structural Plasticity. Neuron 87, 63–75 (2015). [PubMed: 26139370]

43. Ghosh M, et al. Cofilin promotes actin polymerization and defines the direction of cell motility. Science 304, 743–746 (2004). [PubMed: 15118165]

44. Yasuda R. Biophysics of Biochemical Signaling in Dendritic Spines: Implications in Synaptic Plasticity. Biophysical journal 113, 2152–2159 (2017). [PubMed: 28866426]

45. Obashi K, Matsuda A, Inoue Y. & Okabe S. Precise Temporal Regulation of Molecular Diffusion within Dendritic Spines by Actin Polymers during Structural Plasticity. Cell reports 27, 1503–1515.e1508 (2019). [PubMed: 31042476]

46. Wells AM, et al. Extracellular signal-regulated kinase in the basolateral amygdala, but not the nucleus accumbens core, is critical for context-response-cocaine memory reconsolidation in rats. Neuropsychopharmacology 38, 753–762 (2013). [PubMed: 23232446]

47. Theberge FRM, Milton AL, Belin D, Lee JLC & Everitt BJ The basolateral amygdala and nucleus accumbens core mediate dissociable aspects of drug memory reconsolidation. Learning & Memory 17, 444–453 (2010). [PubMed: 20802017]

48. Everitt BJ & Robbins TW Neural systems of reinforcement for drug addiction: from actions to habits to compulsion. Nature Neuroscience 8, 1481–1489 (2005). [PubMed: 16251991]

49. Taylor JR, Olausson P, Quinn JJ & Torregrossa MM Targeting extinction and reconsolidation mechanisms to combat the impact of drug cues on addiction. Neuropharmacology, 1–10 (2008).

50. Wang S-H, de Oliveira Alvares L. & Nader K. Cellular and systems mechanisms of memory strength as a constraint on auditory fear reconsolidation. Nature Neuroscience 12, 905–912 (2009). [PubMed: 19543280]

Methods-only References

51. Mu P, et al. Exposure to cocaine dynamically regulates the intrinsic membrane excitability of nucleus accumbens neurons. J Neurosci 30, 3689–3699 (2010). [PubMed: 20220002]

52. Brebner K, et al. Nucleus accumbens long-term depression and the expression of behavioral sensitization. Science 310, 1340–1343 (2005). [PubMed: 16311338]

53. Mardilovich K, et al. LIM kinase inhibitors disrupt mitotic microtubule organization and impair tumor cell proliferation. Oncotarget 6, 38469–38486 (2015). [PubMed: 26540348]

54. LaPlant Q, et al. Dnmt3a regulates emotional behavior and spine plasticity in the nucleus accumbens. Nature Neuroscience 13, 1137–1143 (2010). [PubMed: 20729844]

55. Maze I, et al. Essential role of the histone methyltransferase G9a in cocaine-induced plasticity. Science 327, 213–216 (2010). [PubMed: 20056891]

56. Barrot M, et al. CREB activity in the nucleus accumbens shell controls gating of behavioral responses to emotional stimuli. Proceedings of the National Academy of Sciences 99, 11435–11440 (2002).

57. Yu J, et al. Nucleus accumbens feedforward inhibition circuit promotes cocaine self-administration. Proceedings of the National Academy of Sciences of the United States of America 56, 201707822 (2017).

58. Huang YH, Schluter OM & Dong Y. Silent Synapses Speak Up: Updates of the Neural Rejuvenation Hypothesis of Drug Addiction. Neuroscientist 21, 451–459 (2015). [PubMed: 25829364]

59. Winters BD, et al. Cannabinoid receptor 1-expressing neurons in the nucleus accumbens. Proceedings of the National Academy of Sciences of the United States of America 109, E2717–2725 (2012). [PubMed: 23012412]

60. Dumitriu D, Rodriguez A. & Morrison JH High-throughput, detailed, cell-specific neuroanatomy of dendritic spines using microinjection and confocal microscopy. Nature protocols 6, 1391–1411 (2011). [PubMed: 21886104]

61. Dumitriu D, et al. Subregional, dendritic compartment, and spine subtype specificity in cocaine regulation of dendritic spines in the nucleus accumbens. The Journal of neuroscience : the official journal of the Society for Neuroscience 32, 6957–6966 (2012). [PubMed: 22593064]

62. Robinson TE & Kolb B. Alterations in the morphology of dendrites and dendritic spines in the nucleus accumbens and prefrontal cortex following repeated treatment with amphetamine or cocaine. 11, 1598–1604 (1999). [PubMed: 10215912]
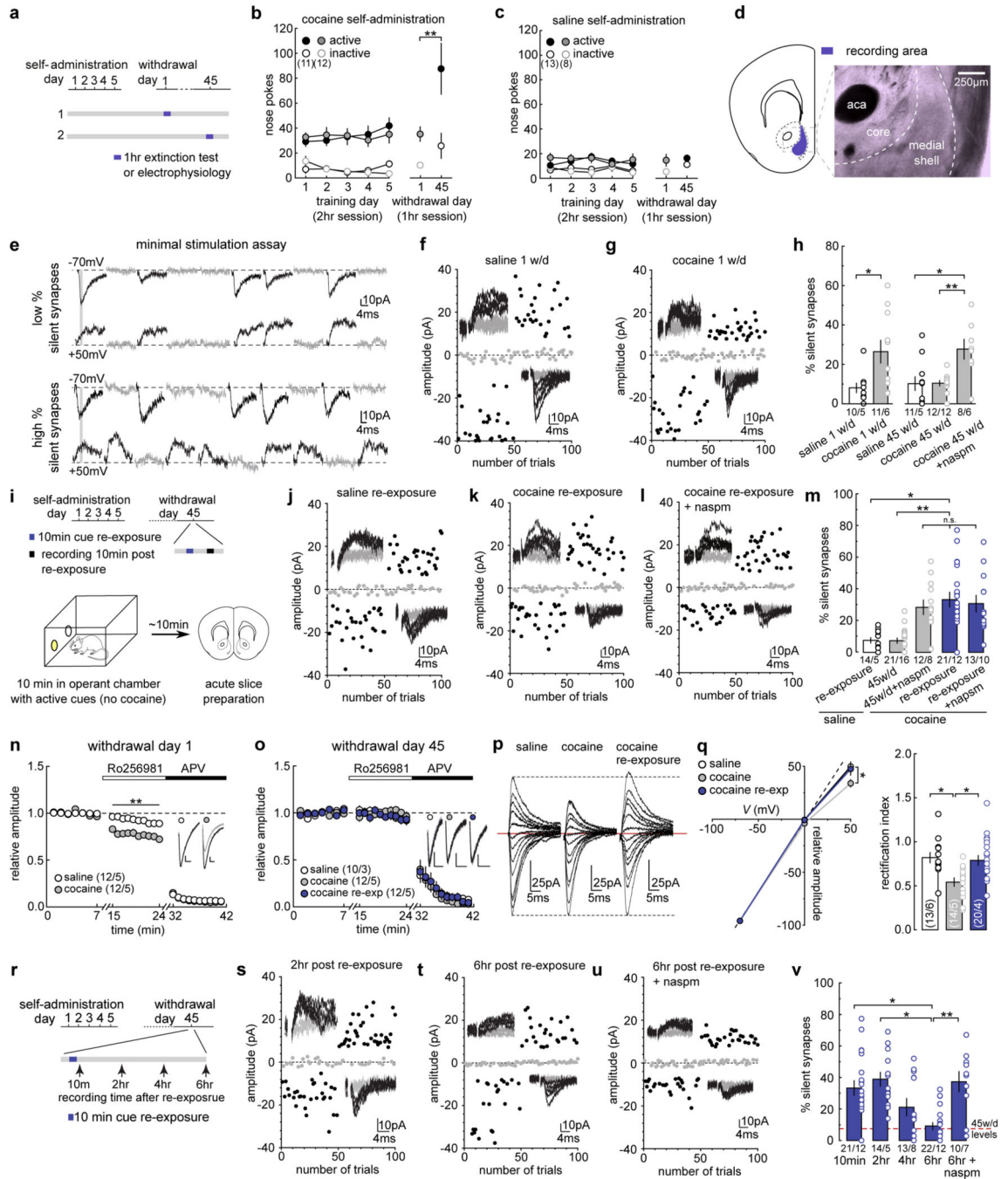
Figure 1. Memory retrieval re-silences cocaine-generated synapses

(a) Diagram showing experimental timeline.

(b and c) Summary showing that after cocaine (b), but not saline (c), self-administration, cue-induced seeking was higher on withdrawal day 45 than withdrawal day 1 (withdrawal day 1 active = 3.08 ± 5.787, n = 12; withdrawal day 45 active = 87.13 ± 20.367, n = 11, $F_{1,38}$=12.27, p=0.0012, two-way ANOVA; **p<0.01, Bonferroni posttest).

(d) Diagram showing the recording area.

(e) Example EPSCs in the minimal stimulation assay, in which failed and successful responses were readily discernable at both −70 mV and +50 mV, and the small vs. large failure rate differences between these two holding potentials connotes low % (upper) vs. high % silent synapses.

(f and g) EPSCs evoked at −70 mV or +50 mV (insets) over 100 trials from example recordings 1 day after saline (f) or cocaine (g) self-administration.

(h) Summary showing that the % silent synapses was increased on withdrawal day 1 after cocaine self-administration (saline = 5.93 ± 1.44, n = 5 animals; cocaine = 24.95 ± 7.13, n = 6 animals, t_9=2.38, p=0.04, two-tail unpaired t-test). On withdrawal day 45, the % silent synapses returned to basal levels, while CP-AMPAR inhibition restored the high % silent synapses (saline = 11.71 ± 5.35, n =5 animals; cocaine = 10.53 ± 1.49, n = 12 animals; cocaine naspm = 28.37 ± 4.68, n = 6 animals, $F_{2,19}$=8.61, p=0.0022, one-way ANOVA; *p<0.05, **p<0.01, Bonferroni posttest).

(i) Diagram showing experimental timeline.

(j-l) EPSCs evoked at −70 mV or +50 mV by minimal stimulation (insets) over 100 trials from example recordings after cue re-exposure from saline- (j) and cocaine-trained rats (k) in the absence or presence (l) of naspm.

(m) Summary showing that cue re-exposure increased the % silent synapses in cocaine-trained, but not saline-trained, rats on withdrawal day 45, and the effects of naspm (saline re-exp = 7.74 ± 1.89, n = 5 animals; cocaine 45w/d = 8.01 ± 1.89, n = 16 animals; cocaine 45w/d naspm = 31.31 ± 5.22, n = 8 animals; cocaine re-exp = 32.89 ± 5.41, n = 12 animals; cocaine re-exp naspm = 29.74 ± 3.85, n = 10, $F_{4,47}$=10.11, p<0.0001, one-way ANOVA; n.s.>0.05 *p<0.05, **p<0.01, Bonferroni posttest).

(n) Summary showing increased sensitivity to Ro256981 of NMDAR EPSCs in rats 1 day after cocaine self-administration (saline = 0.91 ± 0.03 at 24min, n = 5 animals; cocaine = 0.74 ± 0.03 at 24min, n = 5 animals, $F_{26,104}$=7.66, p<0.0001, two-way ANOVA repeated measure; **p<0.01, Bonferroni posttest). Subsequent application of APV (50 μM) confirmed that currents were mediated by NMDARs. Inset showing example NMDAR EPSCs before and during Ro256981 application.

(o) Summary showing cue re-exposure did not affect the Ro256981 sensitivity of NMDAR EPSCs in NAcSh MSNs (saline = 0.93 ± 0.03 at 24min, n =3 animals; cocaine = 0.92 ± 0.06 at 24min, n = 5 animals; cocaine re-exp = 0.93 ± 0.05 at 24min, n = 5, $F_{52,260}$=0.50, p=0.9984, two-way ANOVA repeated measures).

(p) Example AMPAR EPSCs evoked from holding potentials of −70 mV to +50 mV with 10 mV increments.

(q) (Left) *I-V* curves of AMPAR EPSCs showing rectification in cocaine-trained rats on withdrawal day 45, and the rectification was abolished by cue re-exposure (saline = 52.51 ± 5.68, n = 6 animals; cocaine = 29.98 ± 3.17, n = 5 animals; cocaine re-exp = 43.93 ± 6.01, n = 4 animals, $F_{4,33}$=4.15, p=0.0078, two-way ANOVA; *p< 0.05, Bonferroni posttest). EPSC amplitudes at −70 mV were used to normalize EPSCs at other membrane potentials. (Right) Summary showing that on withdrawal day 45, the decreased rectification index in cocaine-trained rats was abolished by cue re-exposure (saline = 0.79 ± 0.051, n = 6 animals; cocaine = 0.54 ± 0.041, n = 5 animals; cocaine re-exp = 0.79 ± 0.057, n = 4 animals, $F_{2,12}$=8.06, p=0.006, one-way ANOVA; *p < 0.05, Bonferroni posttest).

(r) Diagram showing the timepoints at which the effects of cue re-exposure on silent synapses were assessed.

(s-u) EPSCs evoked at −70 mV or +50 mV by minimal stimulation (insets) over 100 trials from example recordings 2 (o) and 6 hr (p) after cue re-exposure in cocaine-trained rats, and 6 hr after re-exposure in the presence of naspm (q).

(v) Summary showing that after cue re-exposure, % silent synapse was immediately increased, remained at high levels for a few hr, and declined to basal levels by ~6 hr, and the declined % silent synapses were restored to high levels by naspm (10-min = 32.89 ± 5.404, n = 12 animals; 2hr = 37.23 ± 4.86, n = 5 animals; 4hr = 23.62 ± 7.78, n = 8 animals; 6hr = 10.91 ± 3.07, n = 12 animals; 6hr naspm = 39.47 ± 5.77, n = 7, $F_{4,39}$=5.02, p=0.0023, one-way ANOVA; *p<0.05, **p<0.01, Bonferroni posttest). The 10-min data taken from m. See Supplemental Table 1 for exact p values for all comparisons made during posthoc tests. Data presented as mean±SEM.
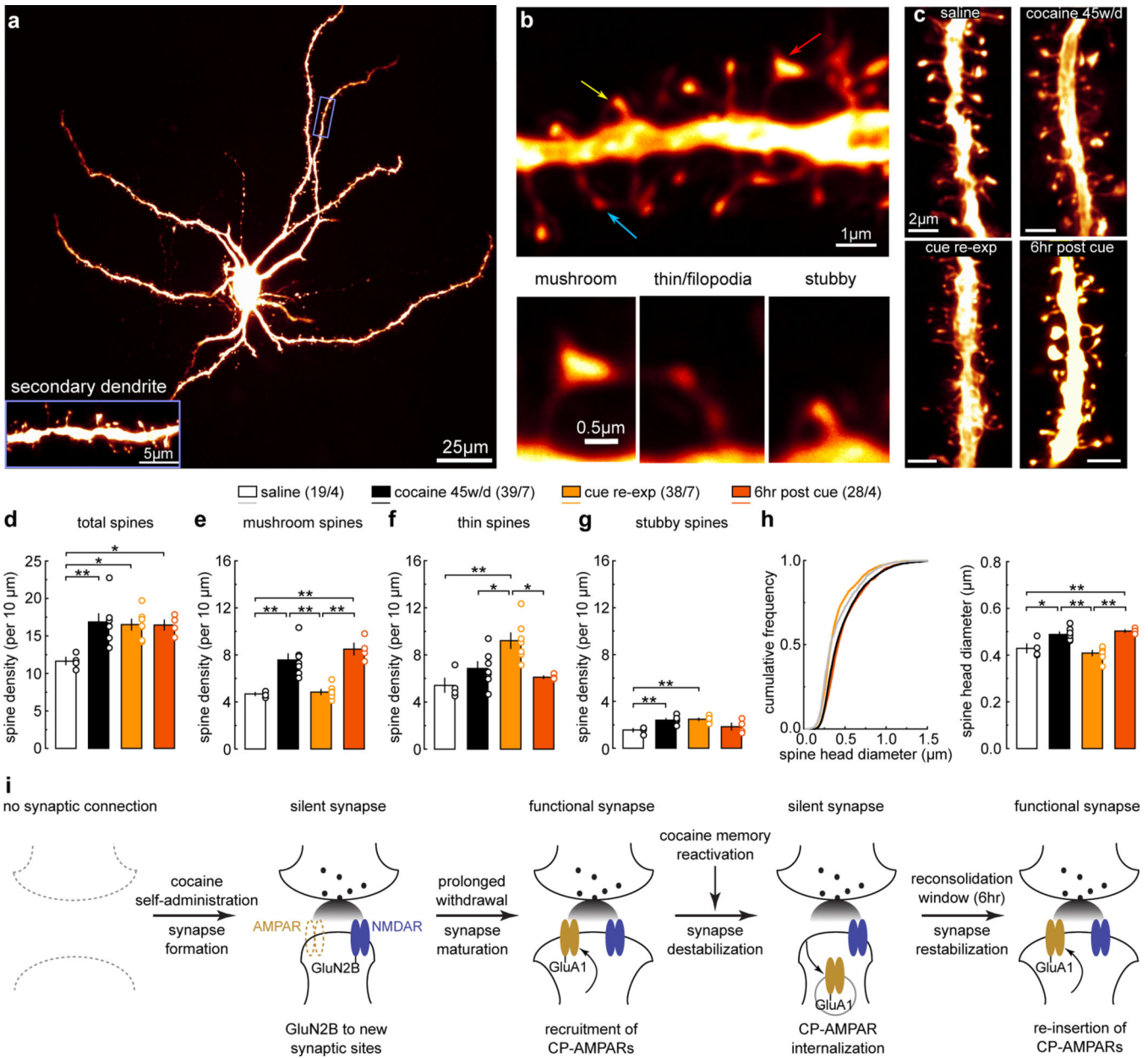
Figure 2. Spine morphology correlate with memory destabilization and reconsolidation

(a) Example image showing a NAcSh MSN filled with Alexa 594 dye, and a magnified secondary dendrite (inset). Replicates for each group are presented in d-h with n values.

(b) Example spiny dendrites (upper) and three subtypes of spines (lower) whose dendritic locations are indicated by arrows; mushroom (red), thin (blue), and stubby (yellow). Replicates for each group are presented in d-h with n values.

(c) Example NAcSh dendrites from saline-trained rats with cue re-exposure (upper left), cocaine-trained rats without (upper right), 10 min after (lower left), and 6hr after (lower right) cue re-exposure on withdrawal day 45. Replicates for each group are presented in d-h with n values.

(d) Summary showing that the density of total spines was increased after 45 days of withdrawal from cocaine compared to saline controls, and this increase was not altered by cue re-exposure and reconsolidation (saline = 11.66 ± 0.49, n = 4 animal; cocaine 45w/d = 16.86 ± 1.12, n = 7 animals; cocaine re-exp = 16.53 ± 0.716, n = 7 animals; cocaine 6hr post = 16.46 ± 0.665, n = 4 animals, $F_{3,18}$=5.98, p=0.0051, one-way ANOVA; *p< 0.05, **p<0.01, Bonferroni posttest).

(e) Summary showing that the density of mushroom-like spines was increased after 45 days of withdrawal from cocaine compared to saline controls. Cue re-exposure decreased mushroom-like spine density to saline levels, while this cue re-exposure-induced effect disappeared 6 hr later (saline = 4.68 ± 0.129, n =4; cocaine 45w/d = 7.57 ± 0.531, n =7; cocaine re-exp = 4.84 ± 0.215, n =7; cocaine 6hr post = 8.50 ± 0.493, n =4, $F_{3,18}$=19.86, p<0.0001; one-way ANOVA; **p<0.01, Bonferroni posttest).

(f) Summary showing that the density of thin spines was increased by cue re-exposure in cocaine-trained rats compared to saline-trained rats or cocaine-rats without re-exposure. Density of thin spines normalized 6 hr after re-exposure (saline = 5.43 ± 0.598, n =4 animals; cocaine 45w/d = 6.86 ± 0.568, n =7 animals; cocaine re-exp = 9.21 ± 0.643, n =7 animals; cocaine 6hr post = 6.12 ± 0.107, n = 4 animals, $F_{3,18}$=7.89, p=0.0014, one-way ANOVA; *p<0.05, **p<0.01, Bonferroni posttest).

(g) Summary showing that the density of stubby spines was increased in cocaine-trained rats with or without cue re-exp, compared to saline-trained rats (saline = 1.56 ± 0.142, n = 4 animals; cocaine 45w/d = 2.41 ± 0.115, n = 7 animals; cocaine re-exposure = 2.47 ± 0.09, n = 7 animals; cocaine 6hr post = 1.85 ± 0.295, n = 4 animals, $F_{3,18}$=8.28, p=0.001, one-way ANOVA; **p<0.01, Bonferroni posttest).

(h) Summary of cumulative frequency (left) and mean values (right) showing an increase in the overall spine head diameter in cocaine-trained rats compared to saline controls. Spine head diameter in cocaine-trained rats decreased to saline levels after cue re-exposure, which normalized 6 hr after re-exposure (saline = 0.429 ± 0.019, n = 4 animals; cocaine 45w/d = 0.488 ± 0.011, n = 7 animals; cocaine re-exp = 0.401 ± 0.011, n = 7 animals; cocaine 6hr post = 0.503 ± 0.005, n = 4 animals, $F_{3,18}$=14.67, p<0.0001, one-way ANOVA; *p<0.05, **p<0.01, Bonferroni posttest).

(i) Schematic illustration depicting the hypothesized dynamics of cocaine-generated silent synapses during acquisition, consolidation, destabilization, and reconsolidation of cocaine-associated memories. See Supplemental Table 1 for exact p values for all comparisons made during posthoc tests. Data presented as mean±SEM.
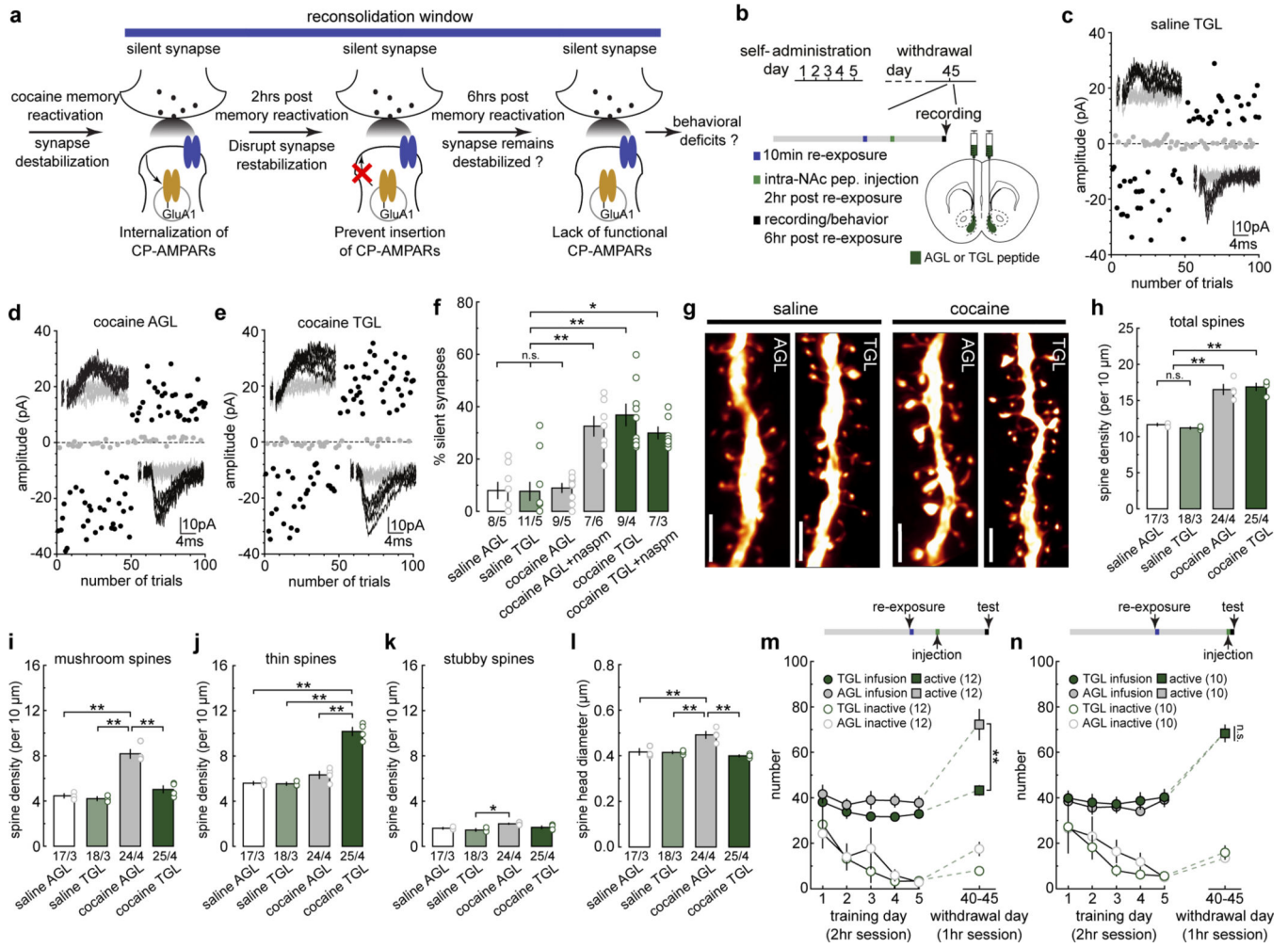
Figure 3. Synapse re-silencing destabilizes cocaine memories

(a) Diagram illustrating the hypothesis that preventing CP-AMPAR re-insertion during the reconsolidation window locks cocaine-generated synapses in the silent state and compromises cue-induced cocaine seeking.

(b) Diagram showing experimental timeline.

(d-e) Example EPSCs evoked at −70 mV and +50 mV by minimal stimulation (insets) over 100 trials from saline- or cocaine-trained rats with NAcSh TGL infusion and the effects of naspm.

(f) Summary showing that while intra-NAcSh TGL or AGL did not affect the % silent synapses in saline-trained rats, intra-NAcSh TGL, but not AGL, maintained the cue re-exposure-induced high % silent synapses in cocaine-trained rats beyond the presumable 6-hr destabilization window, and CP-AMPAR inhibition by naspm did not further affect the % silent synapses (saline AGL = 6.40 ± 3.68, n = 5 animals; saline TGL = 7.06 ± 3.07, n = 5 animals; cocaine AGL = 9.70 ± 1.05, n = 5 animals; cocaine AGL naspm = 33.76 ± 3.71, n = 6 animals; cocaine TGL = 37.10 ± 3.71, n = 4 animals; cocaine TGL naspm = 29.70 ± 3.08, n = 3 animals, $F_{5,22}$=14.85, p<0.0001, one-way ANOVA; n.s. > 0.05, *p<0.05, **p<0.01, Bonferroni posttest).

(g) Example NAcSh dendrites from saline-trained rats and cocaine-trained rats with AGL and TGL infusions. Scale bar, 2.5 μm.

(h) Summary showing the density of total spines was increased in cocaine-trained rats with either AGL or TGL compared to saline-trained rats (saline AGL = 11.66 ± 0.171, n = 3 animals; saline TGL = 11.20 ± 0.146, n =3 animals; cocaine AGL = 16.52 ± 0.69, n =4 animals; cocaine TGL = 16.89 ± 0.488, n = 4 animals, $F_{3,10}$=36.01, p<0.0001, one-way ANOVA; n.s.>0.05 **p<0.01, Bonferroni posttest).

(i) Summary showing the density of mushroom-like spines was increased in cocaine-trained rats with AGL compared to saline-trained rats, while TGL treatment normalized mushroom-like spine density to saline levels (saline AGL = 4.46 ± 0.19, n = 3 animals; saline TGL = 4.23 ± 0.163, n = 3 animals; cocaine AGL = 8.18 ± 0.383, n = 4 animals; cocaine TGL = 5.04 ± 0.302, n = 4 animals, $F_{3,10}$=38.59, p<0.0001, one-way ANOVA; **p<0.01, Bonferroni posttest).

(j) Summary showing the density of thin spines was significantly increased in cocaine-trained TGL rats compared to cocaine-trained AGL rats or saline-trained rats (saline AGL = 5.60 ± 0.148, n = 3 animals; saline TGL = 5.54 ± 0.132, n = 3 animals; cocaine AGL = 6.33 ± 0.309, n = 4 animals; cocaine TGL = 10.16 ± 0.363, n = 4 animals, $F_{3,10}$=60.80, p<0.0001, one-way ANOVA; **p<0.01, Bonferroni posttest).

(k) Summary showing densities of stubby spines in saline- and cocaine-trained rats with AGL or TGL treatment (saline AGL = 1.60 ± 0.076, n = 3 animals; saline TGL = 1.45 ± 0.117, n = 3 animals; cocaine AGL = 2.01 ± 0.051 n = 4 animals; cocaine TGL = 1.69 ± 0.118, n = 4 animals, $F_{3,10}$=6.32, p=0.0112, one-way ANOVA; *p<0.05, Bonferroni posttest).

(l) Summary showing the mean spine head diameter was increased in cocaine-trained AGL rats compared to saline-trained rats, while TGL treatment normalized this increase to saline control levels (saline AGL = 0.417 ± 0.013, n = 3 animals; saline TGL = 0.415 ± 0.005, n = 3 animals; cocaine AGL = 0.492 ± 0.015, n = 4 animals; cocaine TGL = 0.400 ± 0.004, n = 4 animals, $F_{3,10}$=16.17, p=0.0004, one-way ANOVA; **p<0.01, Bonferroni posttest).

(m) Summary showing that intra-NAcSh infusion of TGL, but not AGL, at 2hr after cue re-exposure decreased cue-induced cocaine seeking in cocaine-trained rats, measured 6 hr after cue re-exposure (AGL active = 72.25 ± 6.68, n = 12 animals; TGL active = 43.25 ± 2.07, n = 12 animals; AGL inactive = 17.58 ± 2.90, n =12 animals; TGL inactive = 7.92 ± 1.34, n =12 animals, $F_{1,22}$=12.26, p=0.002, RM two-way ANOVA, withdrawal day 45 peptide x lever interaction; **p<0.01, Bonferroni posttest).

(n) Summary showing that rats with intra-NAcSh infusion of TGL 6 hr after cue re-exposure exhibited similar cue-induced cocaine seeking as AGL rats measured 6.5 hr after cue re-exposure (AGL active = 68.20 ± 2.87, n = 10 animals; TGL active = 68.20 ± 3.74, n =10 animals; AGL inactive = 13.30 ± 1.69, n = 10 animals; TGL inactive = 15.70 ± 2.94, n = 10 animals, $F_{1,18}$=0.23, p=0.64, RM two-way ANOVA, withdrawal day 45 peptide x lever interaction). See Supplemental Table 1 for exact p values for all comparisons made during posthoc tests. Data presented as mean±SEM.
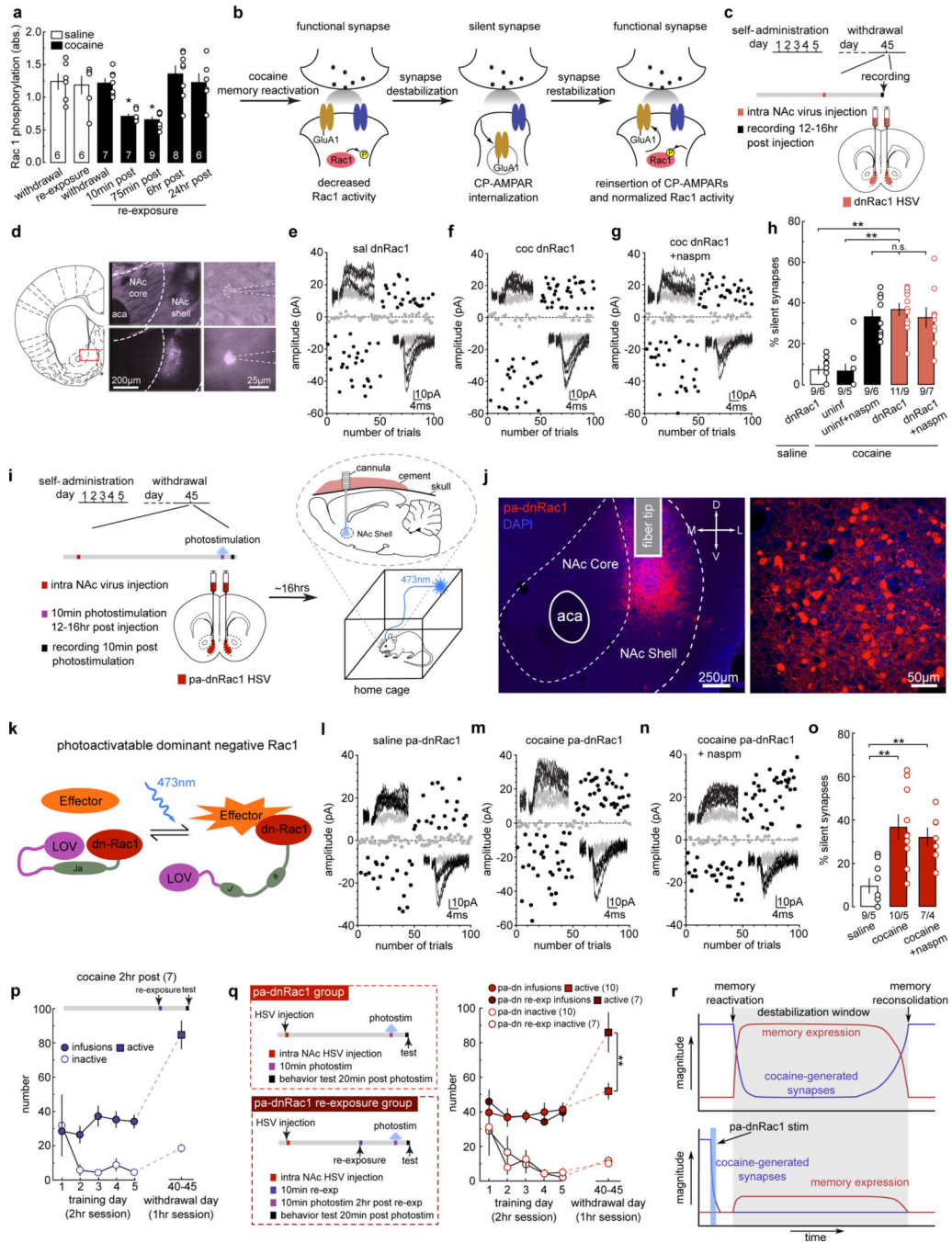
Figure 4. Decreased Rac1 activity primes cue-induced synaptic re-silencing

(a) Summarized ELISA results showing transiently decreased levels of active Rac1 in NAcSh upon cue re-exposure in cocaine-trained but not saline-trained rats (saline withdrawal = 1.24 ± 0.122, n = 6 animals; saline re-exp = 1.19 ± 0.136, n = 6 animals; cocaine withdrawal = 1.23 ± 0.071, n = 7 animals; cocaine 10min = 0.708 ± 0.033, n = 7 animals; cocaine 75min = 0.658 ± 0.041, n = 9 animals; cocaine 6hr = 1.36 ± 0.125, n = 8 animals; cocaine 24hr = 1.23 ± 0.136, n = 6 animals, $F_{6,42}$=, p<0.0001, one-way ANOVA; * p<0.05, Bonferroni posttest).

(b) Diagram illustrating the hypothesis that the transient downregulation of active Rac1 triggers re-silencing of the already matured silent synapses in cocaine-trained rats.

(c) Diagram showing the timeline for experiments involving intra-NAcSh expression of dnRac1.

(d) Example images showing dnRac1-expressing NAcSh MSNs during recordings.

(e-g) EPSCs evoked at −70 mV and +50 mV during the minimal stimulation assay (insets) over 100 trials from example dnRac1-expressing MSNs in saline- (e) and cocaine-trained rats (f), and the effects of naspm (g).

(h) Summary showing that expressing dnRac1 in NAcSh MSNs increased the % silent synapses selectively in cocaine-trained rats on withdrawal day 45, and CP-AMPAR inhibition did not further increase this percentage (saline dnRac1 = 7.32 ± 2.73, n = 6 animals; cocaine non-trans = 6.32 ± 2.59, n = 5 animals; cocaine non-trans naspm = 33.97 ± 4.14, n = 6 animals; cocaine dnRac1 = 36.47 ± 3.46, n = 9 animals; cocaine dnRac1 naspm = 31.67 ± 4.83, n = 7 animals, $F_{2,28}$=14.46, p<0.0001, one-way ANOVA; **p<0.01, Bonferroni posttest).

(i) Diagrams showing the experimental design, in which NAcSh pa-dnRac1 was photoactivated for 10 min while rats remained in their home cage.

(j) Example images of a NAcSh slice (left) and MSNs (right) showing HSV-mediated expression of pa-dnRac1. All animals used in Fig 4o and Fig 4q (n = 26 animals) had pa-dnRac1 expression localized within the NAcSh.

(k) Diagram illustrating the design concept of pa-dnRac1.

(l-n) EPSCs evoked at −70mV and +50mV during the minimal stimulation assay (insets) over 100 trials from example pa-dnRac1-expressing MSNs in saline- (l) and cocaine-trained rats (m), and the effects of naspm (n).

(o) Summary showing that stimulating pa-dnRac1 on withdrawal day 45 did not affect the % silent synapses in saline-trained rats, but increased the % silent synapses in cocaine-trained rats, and this increase was not affected by naspm (saline = 9.08 ± 1.70, n = 5 animals; cocaine = 35.91 ± 4.89, n = 5 animals; cocaine naspm = 33.07 ± 4.21, n = 4 animals, $F_{2,11}$=15.56, p =0.0006, one-way ANOVA; **p<0.01, Bonferroni posttest).

(p) Summary showing that the nose poke responding remained at high levels in cocaine-trained rats when tested 2 hr after cue re-exposure (cocaine 2hr post = 84.86 ± 8.08, n = 7 animals).

(q) (left) Diagrams showing the experimental timeline for cocaine-trained rats that received stimulation of pa-dnRac1 without (upper) and with (lower) prior cue re-exposure. (right) Summary showing that rats that received pa-dnRac1 stimulation without prior cue re-exposure exhibited decreased cue-induced cocaine seeking compared to rats with prior (2 hr before) cue re-exposure (pa-dnRac1 active = 52.00 ± 4.54, n = 10 animals; pa-dnRac1 re-exp active = 85.71 ± 11.23, n = 7 animals; pa-dnRac1 inactive = 10.50 ± 1.17, n = 10 animals; pa-dnRac1 re-exp inactive = 12.14 ± 2.01, n = 7 animals, $F_{1,15}$=9.17, p=0.0085, RM two-way ANOVA, withdrawal day 45 lever x group interaction; **p<0.01, Bonferroni posttest).

(r) Hypothetical diagrams illustrating the dissociation between the functional state of cocaine-generated synapses and the behavioral expression (seeking) following reactivation of cocaine memories. *Upper*: after cue re-exposure-induced memory reactivation, cocaine-generated synapses are re-silenced, while cocaine seeking remains at high levels for a few hr. *Lower*: when cocaine-generated synapses are re-silenced and weakened beforehand, cue

re-exposure does not induce high-level cocaine seeking. Thus, cocaine-generated silent synapses involve in the storage or reactivation of cocaine memories, while cocaine seeking expressed during the memory destabilization window is driven by an independent mechanism. See Supplemental Table 1 for exact p values for all comparisons made during posthoc tests. Data presented as mean±SEM.
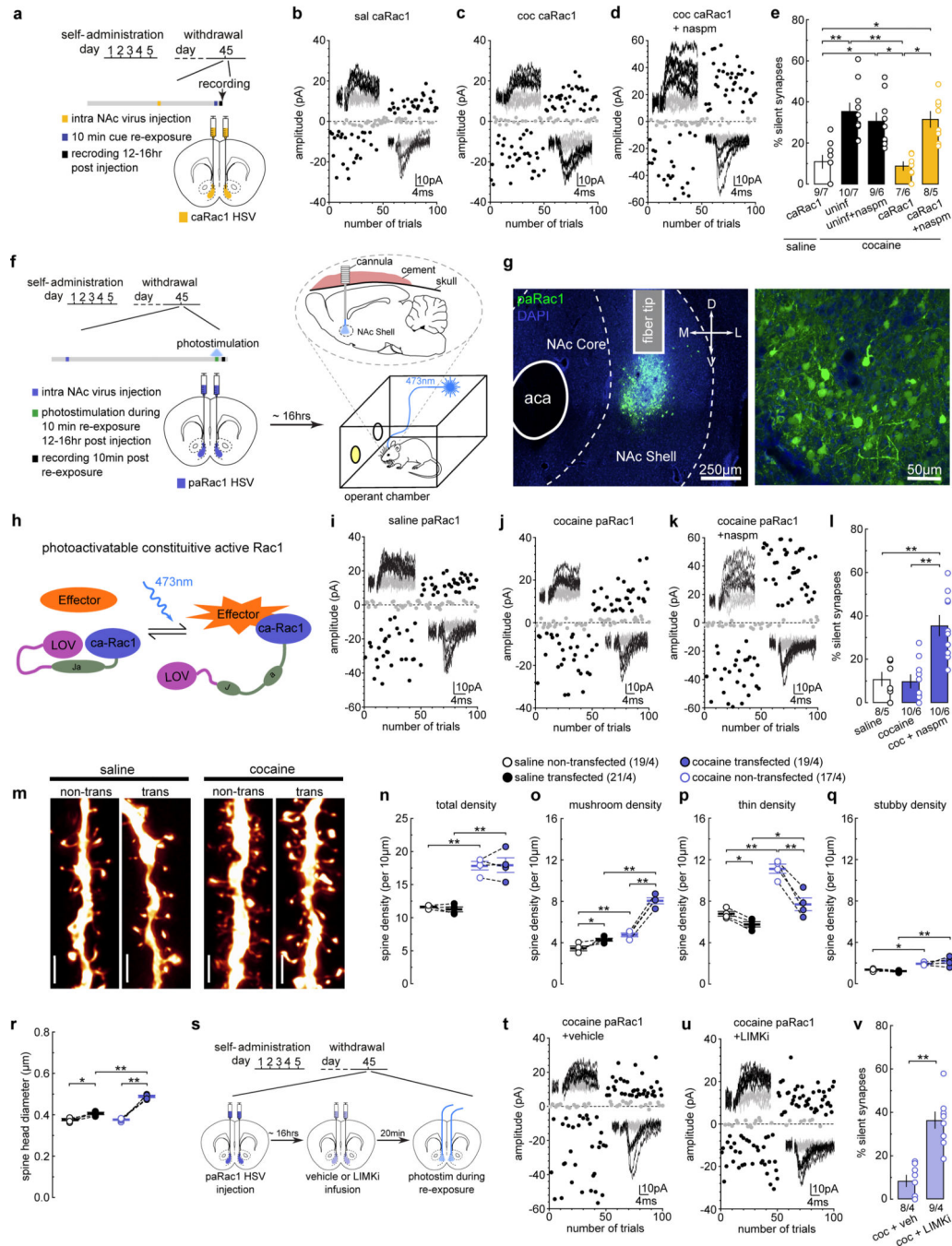
Figure 5. Increasing Rac1 activity prevents cue-induced synaptic re-silencing

(a) Diagram showing the experimental timeline.

(b-d) Example EPSCs evoked at −70mV and +50mV during the minimal stimulation assay (insets) over 100 trials from example caRac1-expressing MSNs in saline- (b), and cocaine-trained rats (c), and the effects of naspm (d).

(e) Summary showing that caRac1 expression prevented the cue re-exposure-induced increase in the % silent synapses in cocaine-trained rats after 45 days of withdrawal from self-administration, while perfusion of naspm restored this % to high levels (saline caRac1 =

10.34 ± 2.90, n = 7 animals; cocaine non-trans = 37.22 ± 5.40, n = 7 animals; cocaine non-trans naspm = 27.94 ± 4.94, n = 6 animals; cocaine caRac1 = 8.49 ± 2.10, n =6 animals; cocaine caRac1 naspm = 30.76 ± 3.17, n = 5 animals, $F_{4,26}$=10.44, p<0.0001, one-way ANOVA; *p<0.05, **p<0.01, Bonferroni posttest).

(f) Diagrams showing the experimental design, in which NAcSh pa-Rac1 was photoactivated during the 10 min cue re-exposure in rats on withdrawal day 45.

(g) Example images of a NAcSh slice (left) and MSNs (right) showing HSV-mediated expression of paRac1. All animals used in Fig 5l, Fig 5n-r, Fig 5v, and Fig 6q (n = 41 animals) had pa-dnRac1 expression localized within the NAcSh.

(h) Diagram illustrating the design concept of paRac1.

(i-k) EPSCs evoked at −70mV and +50mV during the minimal stimulation assay (insets) over 100 trials from example paRac1-expressing MSNs in saline- (i) and cocaine-trianed rats (j), and the effects of naspm (k).

(l) Summary showing that stimulating paRac1 during cue re-exposure prevented cue re-exposure-induced re-silencing of the matured silent synapses in cocaine-trained rats, which was revealed by perfusion of naspm; paRac1 stimulation did not affect the % silent synapses in saline-trained rats (saline = 12.32 ± 2.74, n = 5 animals; cocaine = 9.39 ± 2.81, n = 6 animals; cocaine naspm = 34.83 ± 5.09, n = 6 animals, $F_{2,14}$=13.74, p=0.0005, one-way ANOVA; **p<0.01, Bonferroni posttest).

(m) Example NAcSh dendrites of MSNs without and without paRac1 expression from saline-trained rats and cocaine-trained rats with photostimulation during cue re-exposure. Scale bar, 2.5 μm.

(n) Summary showing that the total spine density was increased in cocaine-trained rats after cue re-exposure for both non-transduced and transduced MSNs compared to saline-trained rats (saline non-trans = 11.62 ± 0.138, n = 4 animals; saline trans = 11.23 ± 0.363, n = 4 animals; cocaine non-trans = 17.83 ± 0.631, n = 4 animals; cocaine trans = 17.94 ± 1.11, n =4 animals, $F_{1,6}$=55.47, p=0.0003, RM two-way ANOVA, drug main effect; **p<0.01, Bonferroni posttest).

(o) Summary showing the increased density of mushroom-like spines was preserved in pcRac1-expressing MSNs from cocaine-trained rats after cue re-exposure, while the density in non-transduced MSNs decreased. paRac1 stimulation also led to a small, but significant increase in mushroom-like spine density in saline-trained rats (saline non-trans = 3.46 ± 0.216, n = 4 animals; saline trans = 4.28 ± 0.140, n = 4 animals; cocaine non-trans = 4.77 ± 0.175, n = 4 animals; cocaine trans = 8.04 ± 0.295, n =4 animals, $F_{1,6}$=57.03, p=0.0003, RM two-way ANOVA, drug x transduced interaction; *p<0.05, **p<0.01, Bonferroni posttest).

(p) Summary showing the decreased density of thin spines was preserved in paRac1-expressing MSNs from cocaine-trained rats after cue re-exposure, while the density in non-transduced MSNs increased. paRac1 stimulation also led to a small, but significant decrease in thin spine density in saline-trained rats (saline non-trans = 6.80 ± 0.230, n = 4 animals; saline trans = 5.76 ± 0.253, n = 4 animals; cocaine non-trans = 11.12 ± 0.439, n = 4 animals; cocaine trans = 7.70 ± 0.618, n =4 animals, $F_{1,6}$=30.88, p=0.0014, RM two-way ANOVA, drug x transduced interaction; *p<0.05, **p<0.01, Bonferroni posttest).

(q) Summary showing the density of stubby spines is increased in cocaine-trained rats after cue re-exposure for both non-transduced and transduced MSNs compared to saline-trained

rats (saline non-trans = 1.37 ± 0.060, n = 4 animals; saline trans = 1.22 ± 0.050, n = 4 animals; cocaine non-trans = 1.95 ± 0.070, n = 4 animals; cocaine trans = 2.20 ± 0.225, n =4 animals, $F_{1,6}$=35.71, p=0.0010, RM two-way ANOVA, drug main effect; *p<0.05, **p<0.01, Bonferroni posttest).

(r) Summary showing the increased mean spine head diameter was preserved in paRac1-expressing MSNs from cocaine-trained rats after cue re-exposure, while the density in non-transduced MSNs normalized back to saline control levels. paRac1 stimulation also led to a small, but significant increase in spine head diameter in saline-trained rats (saline non-trans = 0.375 ± 0.005, n = 4 animals; saline trans = 0.405 ± 0.006, n = 4 animals; cocaine non-trans = 0.377 ± 0.004, n = 4 animals; cocaine trans = 0.488 ± 0.006, n =4 animals, $F_{1,6}$=37.43, p=0.0009, RM two-way ANOVA, drug x transduced interaction; *p<0.05, **p<0.01, Bonferroni posttest).

(s) Diagram showing the experimental timeline for LIMKi experiments.

(t,u) EPSCs evoked at −70mV and +50mV during the minimal stimulation assay (insets) over 100 trials from example paRac1-expressing MSNs from cocaine-trained rats with photostimulation during cue re-exposure with pretreatment of vehicle (t) or LIMKi (u).

(v) Summary showing that pretreatment of LIMKi prevented the effect of paRac1 stimulation on preserving cocaine-generated synapses against re-silencing, such that the % silent synapses were increased compared to vehicle-treated rats (cocaine vehicle = 8.55 ± 1.59, n = 4 animals; cocaine LIMKi = 41.73 ± 6.34, n = 4 animals, t_6=5.08, p=0.0023, two-sided unpaired t-test). See Supplemental Table 1 for exact p values for all comparisons made during posthoc tests. Data presented as mean±SEM.
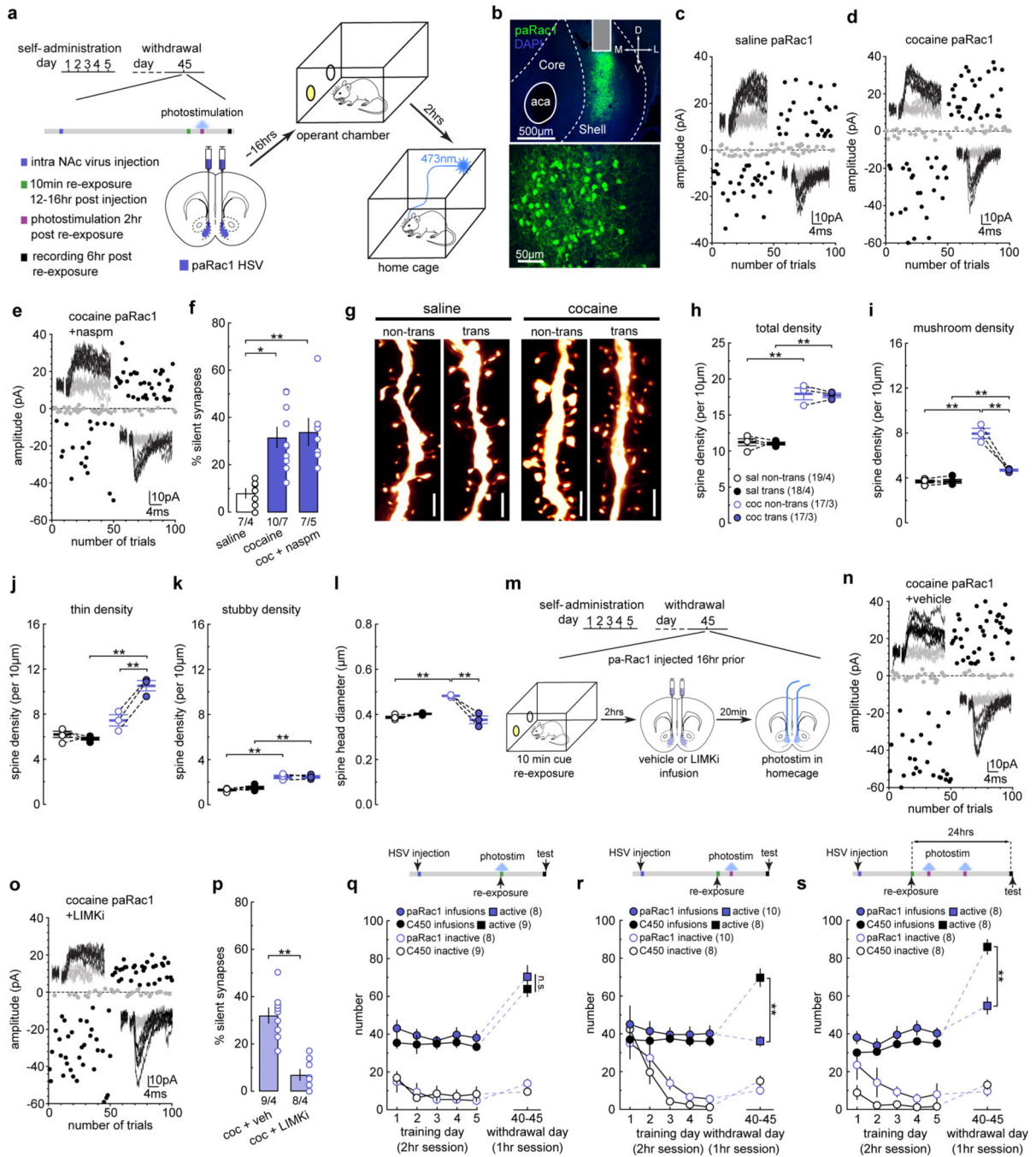
Figure 6. Active Rac1 stabilizes synaptic states to regulate cocaine memory

(a) Diagrams showing the experimental design in which paRac1 is photoactivated 2 hr after cue re-exposure in cocaine-trained rats on withdrawal day 45.

(b) Example images of NAcSh slices (upper) and MSNs (lower) showing HSV-mediated expression of paRac1. All animals used in Fig 6f, Fig 6h-l, Fig 6p, and Fig 6r,s (n = 49 animals) had pa-dnRac1 expression localized within the NAcSh.

(c-e) EPSCs evoked at −70mV and +50mV during the minimal stimulation assay (insets) over 100 trials from example NAcSh MSNs with paRac1 photoactivation after cue re-exposure in saline- (c) and cocaine-trained rats (d), and the effects of naspm (e).

(f) Summary showing that stimulating paRac1 after cue re-exposure did not affect the % silent synapses in saline-trained rats, but locked cocaine-generated silent synapses within their silent state in cocaine-trained rats beyond the presumable 6-hr destabilization window, and CPAMPAR inhibition by naspm did not further increase the % silent synapses (saline = 8.30 ± 2.46, n = 4 animals; cocaine = 32.82 ± 3.48, n = 7 animals; cocaine naspm = 36.32 ± 7.65, n =5 animals, $F_{2,13}$=7.64, p=0.0064, one-way ANOVA; *p<0.05, **p<0.01, Bonferroni posttest).

(g) Example NAcSh dendrites of MSNs non-transduced and transduced with paRac1 from saline- and cocaine-trained rats that received photostimulation 2 hr after cue re-exposure. Scale bar, 2.5 μm.

(h) Summary showing the total spine density was increased in cocaine-trained rats 6 hr after cue re-exposure for both non-transduced and transduced MSNs compared to saline-trained rats (saline non-trans = 11.22 ± 0.484, n = 4 animals; saline trans = 11.03 ± 0.199, n = 4 animals; coaine non-trans = 17.88 ± 0.827, n = 3 animals; cocaine trans = 17.67 ± 0.298, n =3 animals, $F_{1,5}$=148.0, p<0.0001, RM two-way ANOVA, drug main effect; **p<0.01, Bonferroni posttest).

(i) Summary showing that the density of mushroom-like spines was decreased in transduced MSNs from cocaine-trained rats 6 hr after cue re-exposure, while the density in non-transduced MSNs remained high (saline non-trans = 3.69 ± 0.130, n = 4 animlas; saline trans = 3.71 ± 0.175, n = 4 animals; cocaine non-trans = 7.96 ± 0.451, n = 3 animals; cocaine trans = 4.69 ± 0.091, n = 3 animals, $F_{1,5}$=58.92, p=0.0006, RM two-way ANOVA, drug x transduction interaction; **p<0.01, Bonferroni posttest).

(j) Summary showing that the density of thin spines was increased in transduced MSNs from cocaine-trained rats 6 hr after cue re-exposure, while the density in non-transduced MSNs returned to the saline control level (saline non-trans = 6.20 ± 0.280, n =4 animals; saline trans = 5.83 ± 0.128, n = 4 animals; cocaine non-trans = 7.45 ± 0.498, n = 3 animals; cocaine trans = 10.53 ± 0.461, n = 3 animals, $F_{1,5}$=55.71, p=0.0007, RM two-way ANOVA, drug x transduction interaction; **p<0.01, Bonferroni posttest).

(k) Summary showing that the density of stubby spines was increased in cocaine-trained rats 6 hr after cue re-exposure for both non-transduced and transduced MSNs compared to saline controls (saline non-trans = 1.32 ± 0.080, n = 4 animals; saline trans = 1.49 ± 0.135, n = 4 animals; cocaine non-trans = 2.47 ± 0.159, n =3 animals; cocaine trans = 2.45 ± 0.120, n = 3 animals, $F_{1,5}$=79.42, p=0.0003, RM two-way ANOVA, drug main effect; **p<0.01, Bonferroni posttest).

(l) Summary showing that the mean spine head diameter was decreased in transduced MSNs from cocaine-trained rats 6 hr after cue re-exposure, while the spine head diameter in non-transduced MSNs remained high (saline non-trans = 0.387 ± 0.005, n = 4 animals; saline trans = 0.402 ± 0.002, n =4 animals; cocaine non-trans = 0.482 ± 0.003, n = 3 animals; cocaine trans = 0.375 ± 0.017, n = 3 animals, $F_{1,5}$=65.19, p=0.0005, RM two-way ANOVA, drug x transduction interaction; **p<0.01, Bonferroni posttest).

(m) Diagram showing the experimental timeline for LIMKi experiments.

(n-o) EPSCs evoked at −70mV and +50mV during the minimal stimulation assay (insets) over 100 trials from example paRac1-expressing MSNs from cocaine-trained rats receiving photostimulation 2 hr after cue re-exposure with pretreatment of vehicle (n) or LIMKi (o).

(p) Summary showing that pretreatment with LIMKi prevented the effect of paRac1 stimulation on keeping cocaine-generated synapses in a silent state, such that the % silent synapses were decreased compared to vehicle-treated rats (cocaine vehicle = 32.52 ± 1.45, n = 4 animals; cocaine LIMKi = 7.02 ± 2.11, n = 4 animals, t_6=9.95, p<0.0001, two-sided, unpaired t-test).

(q) Summary showing that cocaine-trained rats with photostimulation of paRac1 during cue re-exposure exhibited comparable levels of cue-induced cocaine seeking as in C450M control rats, measured 6 hr after cue re-exposure (C450 active = 63.89 ± 4.15, n = 9 animals; pa-Rac1 active = 70.38 ± 6.00, n = 8 animals; C450 inactive = 9.33 ± 1.53, n = 9 animals; pa-Rac1 inactive 13.75 ± 2.20, n = 8 animals, $F_{1,15}$=0.07, p=0.79, RM two-way ANOVA, withdrawal day 45 lever x virus interaction, n.s. >0.05).

(r) Summary showing that cocaine-trained rats with photostimulation of paRac1 2 hr after cue re-exposure exhibited decreased cue-induced cocaine seeking compared to C450M control rats when measured 6 hr after re-exposure (C450 active = 69.88 ± 4.69, n = 8 animals; pa-Rac1 active = 36.20 ± 2.59, n = 10 animals; C450 inactive = 15.13 ± 2.66, n = 8 animals; pa-Rac1 inactive = 10.10 ± 2.15, n = 10 animals, $F_{1,16}$=31.89, p<0.0001, RM two-way ANOVA, withdrawal day 45 lever x virus interaction; **p<0.01, Bonferroni posttest).

(s) Summary showing that cocaine-trained rats with photostimulation of paRac1 2 hr after cue re-exposure exhibited decreased cue-induced cocaine seeking compared to C450M control rats when measured 24 hr after re-exposure (C450 active = 86.13 ± 3.82, n = 8 animals; pa-Rac1 active = 55.88 ± 4.40, n = 8 animals; C450 inactive = 13.00 ± 2.47, n = 8 animals; pa-Rac1 = 9.63 ± 2.61, n = 8 animals, $F_{1,14}$=15.55, p=0.0015, RM two-way ANOVA, withdrawal day 45 lever x virus interaction; **p<0.01, Bonferroni posttest). See Supplemental Table 1 for exact p values for all comparisons made during posthoc tests. Data presented as mean±SEM.